REPORT DOCUMENTATION PAGE

Form Approved OMB NO. 0704-0188

1. REPORT DATE (DD-MM-YYYY)	2. REPORT TYPE	3. DATES COVERED (From - To)
23-12-2013	Final Report	1-Aug-2010 - 30-Sep-2013

4. TITLE AND SUBTITLE
7-Day Biodefense: Engineered Nanoparticle for Virus Elimination by Opsonization (ENVELOP)

5a. CONTRACT NUMBER
W911NF-10-1-0268

5b. GRANT NUMBER

5c. PROGRAM ELEMENT NUMBER
0310BF

6. AUTHORS
James Comolli

5d. PROJECT NUMBER

5e. TASK NUMBER

5f. WORK UNIT NUMBER

7. PERFORMING ORGANIZATION NAMES AND ADDRESSES
The Charles Stark Draper Laboratory, Inc.
555 Technology Square

Cambridge, MA 02139 -3539

8. PERFORMING ORGANIZATION REPORT NUMBER

9. SPONSORING/MONITORING AGENCY NAME(S) AND ADDRESS (ES)
U.S. Army Research Office
P.O. Box 12211
Research Triangle Park, NC 27709-2211

10. SPONSOR/MONITOR'S ACRONYM(S)
ARO

11. SPONSOR/MONITOR'S REPORT NUMBER(S)
58218-LS-DRP.4

12. DISTRIBUTION AVAILIBILITY STATEMENT
Approved for Public Release; Distribution Unlimited

13. SUPPLEMENTARY NOTES
The views, opinions and/or findings contained in this report are those of the author(s) and should not contrued as an official Department of the Army position, policy or decision, unless so designated by other documentation.

14. ABSTRACT
We have developed a technology platform to produce anti-viral particles that block infection by broad classes of respiratory, and other, viruses. The anti-viral particles are composed of liposomes with surface-attached glycan receptors designed so that they mimic the natural human viral receptors and strongly adhere to the virus. On this program, one anti-viral particle designed to counter human-adapted influenza A viruses and another to counter respiratory syncytial (RSV) were produced. Receptor-bearing liposomes were demonstrated to bind to virus with high affinity, block viral infection of cells in culture, and improve survival of animals infected with a lethal dose of

15. SUBJECT TERMS
influenza, respiratory virus, anti-viral, liposome, glycan, receptor, hemagglutinin, sialic acid

16. SECURITY CLASSIFICATION OF:			17. LIMITATION OF ABSTRACT	15. NUMBER OF PAGES	19a. NAME OF RESPONSIBLE PERSON
a. REPORT	b. ABSTRACT	c. THIS PAGE			James Comolli
UU	UU	UU	UU		19b. TELEPHONE NUMBER 617-258-4232

Report Title

7-Day Biodefense: Engineered Nanoparticle for Virus Elimination by Opsonization (ENVELOP)

ABSTRACT

We have developed a technology platform to produce anti-viral particles that block infection by broad classes of respiratory, and other, viruses. The anti-viral particles are composed of liposomes with surface-attached glycan receptors designed so that they mimic the natural human viral receptors and strongly adhere to the virus. On this program, one anti-viral particle designed to counter human-adapted influenza A viruses and another to counter respiratory syncytial (RSV) were produced. Receptor-bearing liposomes were demonstrated to bind to virus with high affinity, block viral infection of cells in culture, and improve survival of animals infected with a lethal dose of virus. In addition we have worked toward production of an aerosolized form that can be delivered to the human respiratory tract to prevent the spread of virus during an outbreak or to treat infected individuals.

Enter List of papers submitted or published that acknowledge ARO support from the start of the project to the date of this printing. List the papers, including journal references, in the following categories:

(a) Papers published in peer-reviewed journals (N/A for none)

Received		Paper
12/20/2013	2.00	G. L. Hendricks, K. L. Weirich, K. Viswanathan, J. Li, Z. H. Shriver, J. Ashour, H. L. Ploegh, E. A. Kurt-Jones, D. K. Fygenson, R. W. Finberg, J. C. Comolli, J. P. Wang. Sialylneolacto-N-tetraose c (LSTc)-bearing Liposomal Decoys Capture Influenza A Virus, Journal of Biological Chemistry, (01 2013): 8061. doi: 10.1074/jbc.M112.437202
TOTAL:		**1**

Number of Papers published in peer-reviewed journals:

(b) Papers published in non-peer-reviewed journals (N/A for none)

Received		Paper
TOTAL:		

Number of Papers published in non peer-reviewed journals:

(c) Presentations

Anti-influenza Activity Of LSTc-labeled Liposomes

Number of Presentations: 1.00

Non Peer-Reviewed Conference Proceeding publications (other than abstracts):

Received Paper

TOTAL:

Number of Non Peer-Reviewed Conference Proceeding publications (other than abstracts):

Peer-Reviewed Conference Proceeding publications (other than abstracts):

Received Paper

TOTAL:

Number of Peer-Reviewed Conference Proceeding publications (other than abstracts):

(d) Manuscripts

Received Paper

TOTAL:

Number of Manuscripts:

Books

Received Paper

TOTAL:

Patents Submitted

Multivalent Liposomal Anti-adhesion Formulations

Identity of oligosaccharides that serve as high affinity receptors for Respiratory Syncytial Virus and their multivalent display

Patents Awarded

Awards

Graduate Students

NAME	PERCENT_SUPPORTED	Discipline
Kevin Yu	1.00	
Gabriel Hendricks	1.00	
Kim Weirich	0.60	
Katya Nacheva	0.40	
FTE Equivalent:	**3.00**	
Total Number:	**4**	

Names of Post Doctorates

NAME	PERCENT_SUPPORTED
Uday Aich	0.50
Jing Li	0.50
FTE Equivalent:	**1.00**
Total Number:	**2**

Names of Faculty Supported

NAME	PERCENT_SUPPORTED	National Academy Member
Robert Finberg	0.20	
Jennifer Wang	0.20	
Evelyn Kurt-Jones	0.10	
Ram Sasisekharan	0.10	
Deborah Fygenson	0.25	
FTE Equivalent:	**0.85**	
Total Number:	**5**	

Names of Under Graduate students supported

NAME	PERCENT_SUPPORTED	Discipline
Olivia Thomas	0.50	Biology
Amita Gupta	0.20	Bioengineering
Lourdes Velasquez	0.50	Physics
Nicole McAllister	0.50	Biology
Kevin Velasquez	0.50	Bioengineering
FTE Equivalent:	**2.20**	
Total Number:	**5**	

Student Metrics

This section only applies to graduating undergraduates supported by this agreement in this reporting period

The number of undergraduates funded by this agreement who graduated during this period:	4.00
The number of undergraduates funded by this agreement who graduated during this period with a degree in science, mathematics, engineering, or technology fields:	5.00
The number of undergraduates funded by your agreement who graduated during this period and will continue to pursue a graduate or Ph.D. degree in science, mathematics, engineering, or technology fields:	4.00
Number of graduating undergraduates who achieved a 3.5 GPA to 4.0 (4.0 max scale):	3.00
Number of graduating undergraduates funded by a DoD funded Center of Excellence grant for Education, Research and Engineering:	0.00
The number of undergraduates funded by your agreement who graduated during this period and intend to work for the Department of Defense	0.00
The number of undergraduates funded by your agreement who graduated during this period and will receive scholarships or fellowships for further studies in science, mathematics, engineering or technology fields:	1.00

Names of Personnel receiving masters degrees

NAME	
Kevin Yu	
Total Number:	**1**

Names of personnel receiving PHDs

NAME	
Gabriel Hendricks	
Kim Weirich	
Total Number:	**2**

Names of other research staff

NAME	PERCENT_SUPPORTED
Shankar Sundaram	0.25
Leila Albers	1.00
Spiros Manalakos	0.50
Theresa Evans-Nguyen	0.20
Amanda Lever	0.20
Chris Palmiotti	0.50
Steve Austin	0.50
Zach Schiller	0.10
Zach Shriver	0.20
Karthik Viswanathan	0.20
Rahul Raman	0.20
FTE Equivalent:	**3.85**
Total Number:	**11**

Sub Contractors (DD882)

1 a. Massachusetts Institute of Technology

1 b. 77 Massachusetts Avenue

Cambridge MA 021394307

Sub Contractor Numbers (c):
Patent Clause Number (d-1):
Patent Date (d-2):
Work Description (e):
Sub Contract Award Date (f-1):
Sub Contract Est Completion Date(f-2):

---

1 a. Massachusetts Institute of Technology

1 b. 77 Massachusetts Avenue

Cambridge MA 021394307

Sub Contractor Numbers (c):
Patent Clause Number (d-1):
Patent Date (d-2):
Work Description (e):
Sub Contract Award Date (f-1):
Sub Contract Est Completion Date(f-2):

---

1 a. University of California - Santa Barbara

1 b. 3227 Cheadle Hall
3rd floor, MC 2050

Santa Barbara CA 931062050

Sub Contractor Numbers (c):
Patent Clause Number (d-1):
Patent Date (d-2):
Work Description (e):
Sub Contract Award Date (f-1):
Sub Contract Est Completion Date(f-2):

---

1 a. University of California - Santa Barbara

1 b. Office Of Research
Cheadle Hall, Room 3227

Santa Barbara CA 931062050

Sub Contractor Numbers (c):
Patent Clause Number (d-1):
Patent Date (d-2):
Work Description (e):
Sub Contract Award Date (f-1):
Sub Contract Est Completion Date(f-2):

1 a. University of Massachusetts Medical School 1 b. 55 Lake Avenue North

Worcester MA 01655

Sub Contractor Numbers (c):

Patent Clause Number (d-1):

Patent Date (d-2):

Work Description (e):

Sub Contract Award Date (f-1):

Sub Contract Est Completion Date(f-2):

Inventions (DD882)

Scientific Progress

This report describes the achievements of a multidisciplinary team from Draper Laboratory, MIT, the University of California – Santa Barbara, and the University of Massachusetts Medical School, on the DARPA/DSO project entitled “Engineered Nanoparticle for Virus Elimination by Opsonization (ENVELOP)”, part of the 7-Day Biodefense program. On this program the team has developed a technology platform to produce broad spectrum anti-viral particles that block infection by respiratory viruses. We have produced two different types of anti-viral particles, one designed to counter human-adapted influenza A viruses and another to counter respiratory syncytial (RSV) and related viruses. These were each demonstrated to block viral infection in cell culture and/or in animal models. Our team has been working to develop and demonstrate an aerosolized form that can be delivered to the human respiratory tract to prevent the spread of virus during an outbreak or to treat infected individuals.

The anti-viral particles are comprised of liposomes with surface-attached glycan receptors that bind virus. The receptors are designed so that they mimic the natural viral receptors in the human airway and adhere to the virus with high affinity. A significant advance was development of a process to identify and synthesize these biomimetic viral receptors. This process, validated with human-adapted influenza A and RSV, can be applied to any group of viruses. Glycan identification was accomplished by combining information about glycans present on target cells, in this case airway epithelial cells, structural analysis of viral binding proteins, and high-throughput glycan array screening of viral specificity. LSTc for human-adapted influenza A and HSocta, a heparin derived octasaccharide, for RSV were selected on the basis of their binding affinity for the virus and for their ease of production/purification. Purified glycans were covalently linked to lipids via one of two glycolipid synthesis processes developed and optimized on the program. Glycan-bearing lipids were formulated into liposomes with DOPC and cholesterol, other lipids that have been used in previously FDA-approved liposomal products. Glycan purification, glycolipid synthesis, and liposome production processes were each tailored so that they are scalable and able to be utilized under GLP or GMP.

LSTc-labeled liposomes inhibited the ability of influenza A to infect cells in vitro with broad influenza specificity, blocking all H1N1 and H3N2 strains tested. A single dose of LSTc-labeled liposomes significantly extended the lifetime of mice infected with the lethal dose of mouse-adapted influenza H1N1, and increased the rate of post-infection survival relative to infected mice that received no liposomes or liposomes lacking LSTc. This indicated that the LSTc on the liposome surface was able to bind to influenza virus in mice and prevent the virus from productively entering airway cells, and demonstrated that the liposome molecule was able to effectively interfere with influenza infection in vivo. Several studies confirmed that the mechanism of action of LSTc-bearing liposomes to be consistent with binding to viral particles and preventing their entry into host cells. Pharmacokinetic studies in mice using radiolabeled LSTc-bearing liposome indicate that liposome reside in the lungs for ~2 days, making prophylaxis possible.

We also demonstrated the platform in developing liposomes bearing receptors for respiratory syncytial virus (RSV). RSV is known to bind heparan sulfate, and we have identified and isolated specific heparan-sulfate derived glycans, conjugated them to DOPE to produce a glycolipid, and produced glycan-bearing liposomes that inhibited RSV infection in vitro. This indicates that the glycan-bearing liposome platform has the potential for broad-reaching anti-viral activity.

Technology Transfer

DARPA 7-Day Biodefense Program

Engineered Nanoparticle for Virus Elimination by Opsonization (ENVELOP)

Final Report

December 10, 2013

James Comolli (PI)
Charles Stark Draper Laboratory, Inc.
555 Technology Square
Cambridge MA 02139

CONTRACT NO: W911NF-10-1-0268

EXECUTIVE SUMMARY

This report describes the achievements of a multidisciplinary team from Draper Laboratory, MIT, the University of California – Santa Barbara, and the University of Massachusetts Medical School, on the DARPA/DSO project entitled "Engineered Nanoparticle for Virus Elimination by Opsonization (ENVELOP)", part of the 7-Day Biodefense program. On this program the team has developed a technology platform to produce broad spectrum anti-viral particles that block infection by respiratory viruses. We have produced two different types of anti-viral particles, one designed to counter human-adapted influenza A viruses and another to counter respiratory syncytial virus (RSV) and related viruses. These were each demonstrated to block viral infection in cell culture and/or in animal models. Our team has been working to develop and demonstrate an aerosolized form that can be delivered to the human respiratory tract to prevent the spread of virus during an outbreak or to treat infected individuals.

The anti-viral particles are comprised of liposomes with surface-attached glycan receptors that bind virus. The receptors are designed so that they mimic the natural viral receptors in the human airway and thus adhere to the virus with high affinity. A significant advance was development of a process to identify and synthesize these biomimetic viral receptors. This process, validated with human-adapted influenza A and RSV, can be applied to any group of viruses. Glycan identification was accomplished by combining information about glycans present on target cells, in this case airway epithelial cells, structural analysis of viral binding proteins, and high-throughput glycan array screening of viral specificity. LSTc for human-adapted influenza A and HSocta, a heparin-derived octasaccharide, for RSV were selected on the basis of their binding affinity for the virus and for their ease of production/purification. Purified glycans were covalently linked to lipids via one of two glycolipid synthesis processes developed and optimized on the program. Glycan-bearing lipids were formulated into liposomes with other lipids that have been used in previously FDA-approved liposomal products. Glycan purification, glycolipid synthesis, and liposome production processes were each tailored so that they are scalable and able to be utilized under GLP or GMP.

LSTc-labeled liposomes inhibited the ability of influenza A to infect cells *in vitro* with broad influenza specificity, blocking all H1N1 and H3N2 strains tested. A single dose of LSTc-labeled liposomes significantly extended the lifetime of mice infected with the lethal dose of mouse-adapted influenza H1N1, and increased the rate of post-infection survival relative to infected mice that received no liposomes or liposomes lacking LSTc. This indicated that the LSTc on the liposome surface was able to bind to influenza virus in mice and prevent the virus from productively entering airway cells, and demonstrated that the liposome molecule was able to effectively interfere with influenza infection *in vivo*. Several studies confirmed that the mechanism of action of LSTc-bearing liposomes to be consistent with binding to viral particles and preventing their entry into host cells. Pharmacokinetic studies in mice using radiolabeled LSTc-bearing liposome indicate that liposome reside in the lungs for 2 to 3 days, making prophylaxis possible.

We also demonstrated the platform in developing liposomes bearing receptors for respiratory syncytial virus (RSV). RSV is known to bind heparan sulfate, and we have identified and isolated specific heparan-sulfate derived glycans, conjugated them to DOPE to produce a glycolipid, and produced glycan-bearing liposomes that inhibited RSV infection *in vitro*. This demonstrated that the glycan-bearing liposome platform has the potential for broad-reaching anti-viral activity that can inhibit the spread of respiratory virus.

TABLE OF CONTENTS

LIST OF FIGURES

LIST OF TABLES

PUBLICATIONS

Hendricks GL, Weirich KL, Viswanathan K, Li J, Shriver ZH, Ashour J, Ploegh HL, Kurt-Jones EA, Fygenson DK, Finberg RW, Comolli JC, Wang JP. Sialylneolacto-N-tetraose c (LSTc)-bearing liposomal decoys capture influenza A virus. J Biol Chem. 2013 Mar 22;288(12):8061-73.

Additional publications in preparation.

INTELLECTUAL PROPERTY

- Base Patent: Decoy Influenza Therapies 20100004195
    - Broadly covers umbrella topology glycans – the active recognition molecules (Owned by MIT, Consortium partner, available for licensing)
- Draper Provisional Patent
    - Multivalent Liposomal Anti-adhesion Formulations - Liposomal formulation and display of glycans allowing for high-efficacy binding and human-safe delivery
- Draper Provisional Patent
    - Identity of oligosaccharides that serve as high affinity receptors for Respiratory Syncytial Virus and their multivalent display

TECHNICAL SUMMARY

Glycan receptor design and purification: Influenza A

Bottoms-up approach: characterization of respiratory tract glycans

The influenza coat glycoprotein hemagglutinin (HA) is a lectin that recognizes specific glycan receptors on the surface of host cells and mediates attachment, viral entry, and membrane fusion events. We identified glycan receptors targeted by influenza using complimentary techniques to characterize glycan diversity at the macro and micro levels. First we took advantage of the expanded utility of lectins by performing co-staining with multiple lectins to understand distribution of α2→6 glycan receptors as a part of N- and O-linked glycoproteins in the human upper respiratory epithelia. Second we isolated glycan receptors from representative upper respiratory tissue/primary cell lines and performed a detailed characterization of the glycan structures using mass spectrometry. Our approach was to bridge the lectin staining of different tissue sections with glycan profiling of representative cells using MALDI-MS and MS/MS (TOF-TOF) analyses for carbohydrate characterization and NMR for linkage information.

To elaborate the diversity of the α2→6 glycans predominantly expressed in the upper respiratory tissues, we co-stained representative human tracheal sections with a panel of well-defined lectins. *Sambucus nigra* agglutinin (SNA-I) is a prototypic lectin that specifically binds to α2→6 glycans, while Jacalin and Concanavalin A (Con A) respectively bind to specific motifs in O-linked (-Galβ1-3GalNAcα- and –GlcNAcβ1-3GalNAcα-) and N-linked (trimannosyl core) glycans. Preliminary lectin staining studies demonstrate a widespread distribution of N-linked α2→6 (on ciliated cells) in contrast to the localized distribution of O-linked α2→6 (on goblet cells) glycans on the apical side of the tracheal section (**Figure 1**). In addition, staining of human tracheal tissue

sections with another lectin, LEL, showed extensive staining on the apical surface of the tracheal tissue points to the distribution of N- and O-linked glycans comprising of long oligosaccharide branches with lactosamine repeats. These glycans are predominantly in the upper respiratory tract while alveolar cells of the deep lung were dominated by glycans bearing α2→3-linked sialic acid.

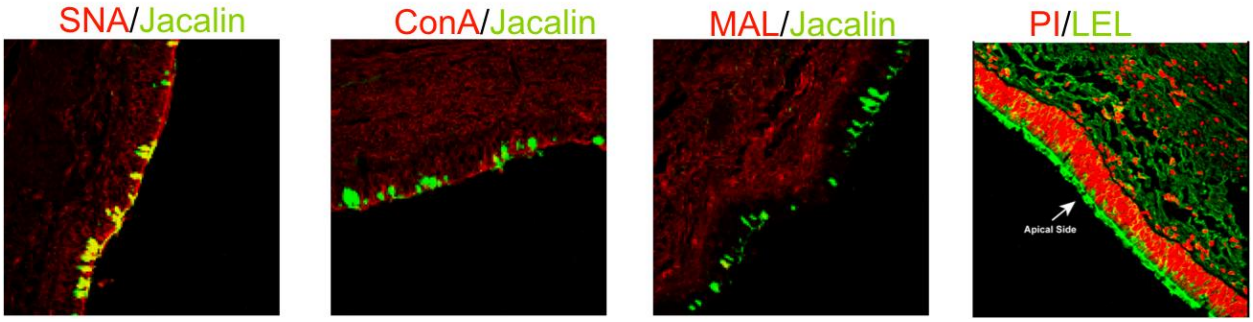

Figure 1. Tracheal and alveolar tissue staining with propodium iodide (nuclei) and the lectin SNA-1 (α2→6 specific) or Maackia Amurensis Lectin II (MAL-II; specific to α2→6 linked sialic acid).

Further 'micro' level characterization was performed by MALDI-MS profiling of N-linked sialylated glycans isolated from a representative human bronchial epithelial (HBE) primary cell line. The MALDI-MS analysis corroborated the lectin staining and showed substantial glycan diversity on human tracheal and bronchial cells as well as the predominant expression of α2→6 glycans. MS/MS analysis of mass peaks further demonstrated the presence of long oligosaccharide branches with multiple lactosamine repeats. The conclusion from these analyses is that human tracheal and bronchial tissue displays higher molecular weight glycans that are long rather than branched, with a predominance of long α2→6-linkages to sialic acid.

Top-down approach: Common structure and topology of glycans targeted by influenza A

The HAs from avian-adapted and human-adapted influenza A strains have been demonstrated to have a binding preference for α2→3 and α2→6-linked sialic acid, respectively, though there are notable exceptions. Using screening of glycan arrays with HAs from various influenza A strains, our team performed a more detailed topological analysis of influenza glycan receptors (**Figure 2**). This revealed common glycan structures preferred by avian- and human-adapted influenza strains, either in the closed (*cone*-like) or open (*umbrella*-like) conformations among the α2→3 and α2→6-linked glycans (**Figure 3**). Binding to either of these configurations can distinguish between avian-adapted and human-adapted influenza strains with 100% accuracy. Long α2→6 sialylated glycans with an umbrella-type topology are those favored by human-adapted strains. These were the same types of glycans found prominent on tracheal and bronchial epithelial cells using bottom-up analysis.

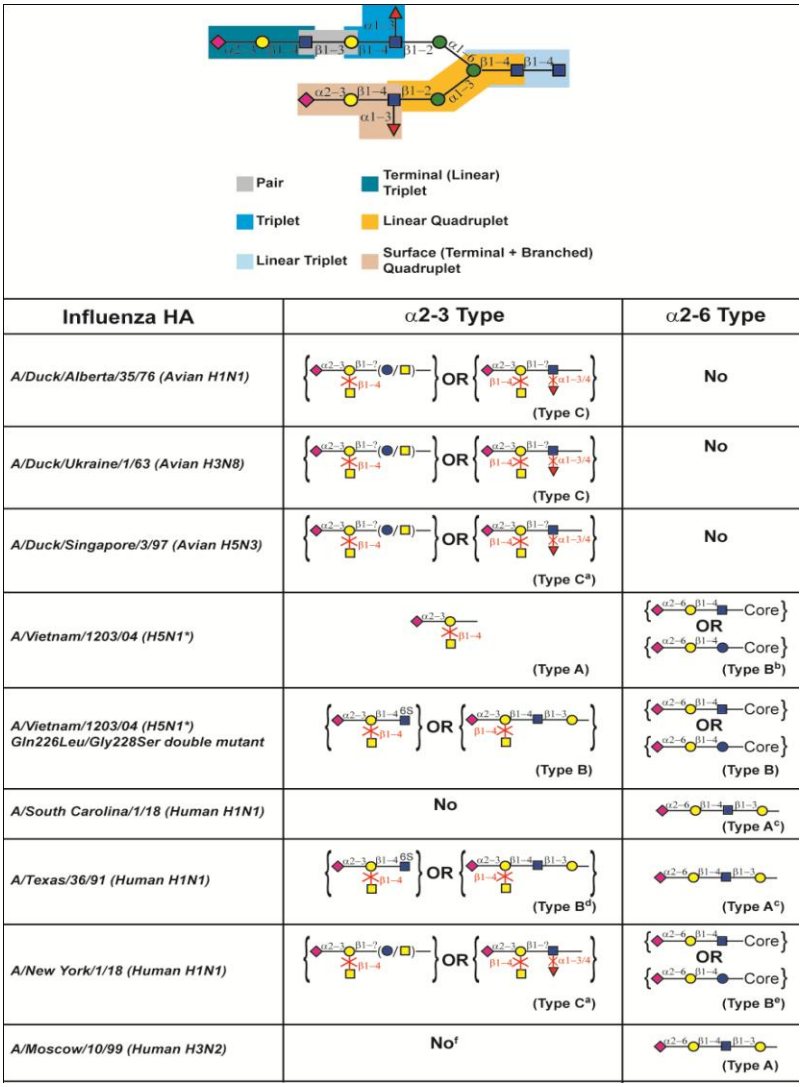

Influenza HA	α2-3 Type	α2-6 Type
A/Duck/Alberta/35/76 (Avian H1N1)	OR (Type C)	No
A/Duck/Ukraine/1/63 (Avian H3N8)	OR (Type C)	No
A/Duck/Singapore/3/97 (Avian H5N3)	OR (Type C[a])	No
A/Vietnam/1203/04 (H5N1)*	(Type A)	Core OR Core (Type B[b])
A/Vietnam/1203/04 (H5N1) Gln226Leu/Gly228Ser double mutant*	OR (Type B)	Core OR Core (Type B)
A/South Carolina/1/18 (Human H1N1)	No	(Type A[c])
A/Texas/36/91 (Human H1N1)	OR (Type B[d])	(Type A[c])
A/New York/1/18 (Human H1N1)	OR (Type C[a])	Core OR Core (Type B[e])
A/Moscow/10/99 (Human H3N2)	No[f]	(Type A)

Figure 2. Glycan receptor preferences of HA from avian-adapted and human-adapted influenza

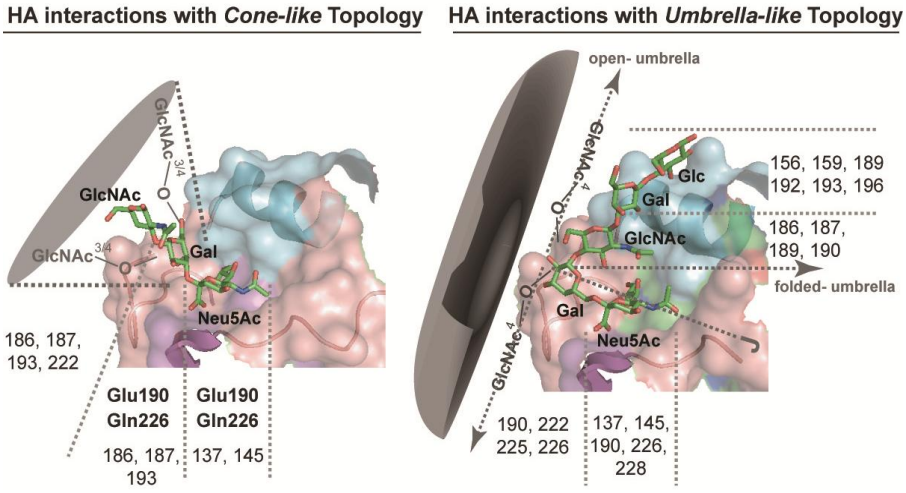

Figure 3. Interaction of cone and umbrella glycan configurations with the receptor binding pocket.

Influenza strains adapted for mouse infection, the animal model used on this project, demonstrate binding to a variety of α2→3 and α2→6 sialylated glycans in both the cone and umbrella conformations. This is demonstrated for the influenza A H1N1 strain PR/8 in a dose-dependent direct binding assay with five defined α2→3 and α2→6 glycans that differ in their surface linkage and length characteristics and represent both *cone*-like and *umbrella*-like topologies. In this study, PR/8 showed the ability to bind both α2→3 and α2→6 linked sialylated glycans with reasonable affinity (**Figure 4**).

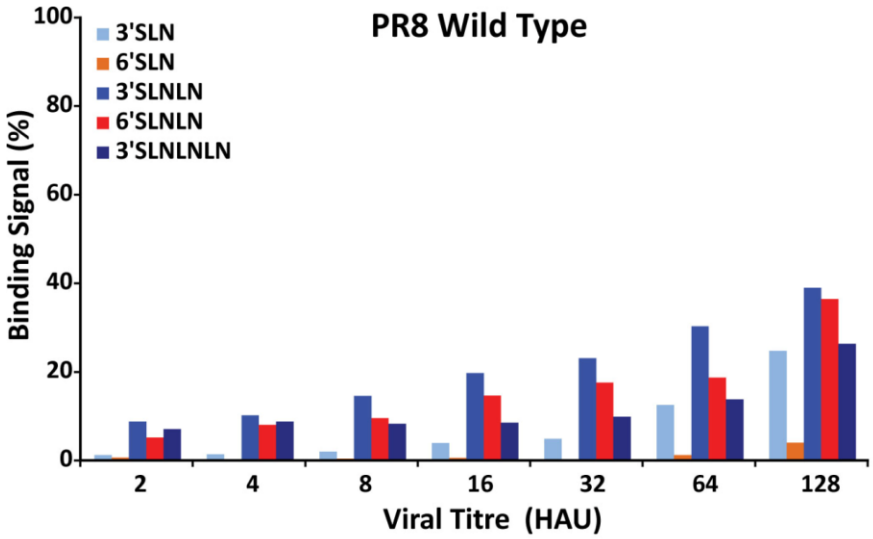

Figure 4. Mixed α2→3 (3') and α2→6 (6') glycan binding of PR/8.

Based on this data and our need to demonstrate efficacy in a mouse model, our initial approach was to construct one liposome displaying an *umbrella*-like topology α2→6 sialylated glycan and another displaying a *cone*-like α2→3 sialylated glycans. These were to be combined to generate a mixture capable of binding and inhibiting PR/8 and other mouse-adapted strains, in addition to a wide range of avian-adapted and human-adapted subtypes. Structural and binding preferences of these strains were integrated and used to identify one cone-like α2→3 sialylated glycan motif and one umbrella-like α2→6 sialylated glycan motif that were bound with high affinity. Glycan selection was also based on demonstrated high-affinity binding to human- or avian-adapted HA subtypes in glycan arrays, and for ease of synthesis and purification. LSTc (Neu5Acα2→6Galβ1→4GlcNAcβ1→3Galβ1→4Glc, α2→6 sialylated, umbrella-like configuration) fits these criteria for binding human-adapted strains, while LSTa (Neu5Acα2→3Galβ1→4GlcNAcβ1→3Galβ1→4Glc, α2→3 sialylated, cone-like configuration) fits the criteria for high affinity binding to avian-adapted strains (**Figure 5**). LSTa and c are present in milk and can be specifically isolated and purified from this plentiful source or chemoenzymatically synthesized. For our studies, free oligosaccharides of LST a/c were separated by gel filtration and high performance liquid chromatography (HPLC) using a normal phase column separation. We successfully obtained ~100 mg of each, and structures were confirmed by proton NMR analysis that matched a reference spectrum for LSTc, specifically the identity of the four distinct monosaccharides and the presence of α2→6 sialic acid at stoichimetric levels.

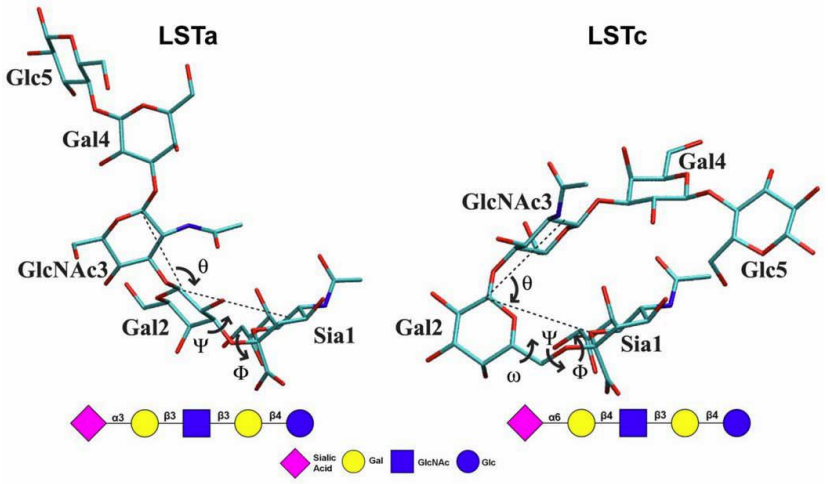

Figure 5. LSTa (α2→3 sialylated, cone-like configuration) and LSTc (α2→6 sialylated, umbrella-like configuration) glycan moieties to be used in liposome formulation.

A quantitative, solid phase assay was used to assess the binding of HA from human- or avian-adapted influenza to LSTa or LSTc. As predicted, HA from a human-adapted H1N1 strains (A/South Carolina/1/18 and A/California/04/2009) demonstrated high affinity binding to LSTc but not LSTa, while A/Vietnam/1194/04, an H5N1 avian-adapted strain, bound to LSTa and not LSTc (**Figure 6**). Further analysis indicated that LSTc binds to human-adapted strains such as SC18 (H1N1) or Alb58 (H2N2) with an apparent affinity of ~5pM. This high-affinity binding is similar to that seen with native α2→6 sialylated, umbrella-like glycans found in the upper respiratory tract.

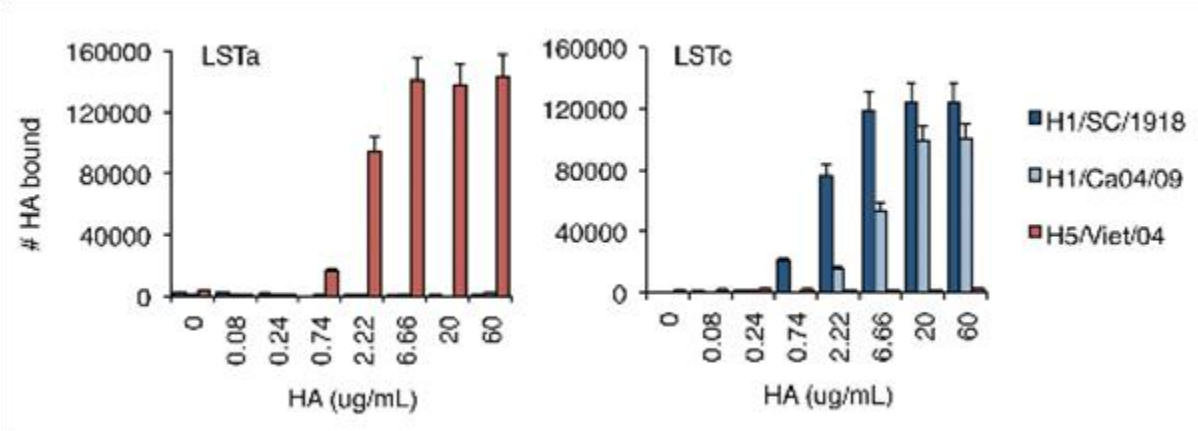

Figure 6. Specificity of LSTc for human-adapted (SC18 and Ca04/09) HA and LSTa for avian-adapted HA (Viet/04).

Glycan receptor design and purification: RSV

To demonstrate the glycan-labeled liposome platform was useful in generating anti-viral particles for respiratory viruses other than influenza, we identified and purified a glycan receptor able to interfere with infection by respiratory syncytial virus (RSV), a major cause of respiratory illness in the newborn infants, young children, the elderly, and severely immunocompromised patients. Our approach to glycan identification was more direct than that used for influenza A. Previous studies definitively demonstrated that cell surface heparan sulfate, a complex highly charged polysaccharide, plays an important role in RSV infection. The RSV

virion directly interacts with cell surface heparan sulfate via its F and G envelope glycoproteins. Importantly, attachment and infectivity of RSV strains was diminished in the presence of soluble heparan sulfate, and removal of cell surface heparan sulfate substantially limited infectivity (Krusat and Streckert, 1997; Feldman et al., 2000). As such, construction of a liposome bearing an oligosaccharide derived from heparan sulfate in a multivalent display was expected to bind to and block RSV infection.

Detailed structural analysis of the F and G proteins identified a putative heparan sulfate binding site. The G protein binding motif is subgroup-dependent [subgroup A (184A→T198) and B (183K → K197)], but constitutes a short, linear peptide that involves a secondary interaction that likely "bridges" with the primary interaction with the F protein. Conversely, the F protein contains a more extended multidomain set of features, including F_1 (^{201}K→I^{217}) and the consensus sequences ^{257}L→S^{287}, ^{327}K→C^{343}, and ^{404}S→T^{434}) and F_2 (represented by ^{33}Y→R^{49} and the consensus sequence ^{54}T→K^{77}). Based on these findings, we reasoned that an octasaccharide is likely able to span the F and G binding sites and serve as the basis for an effective receptor. The proposed octasaccharide receptor is displayed in **Figure 7**.

This particular octasaccharide was chosen for a number of reasons: it has a relatively high charge density

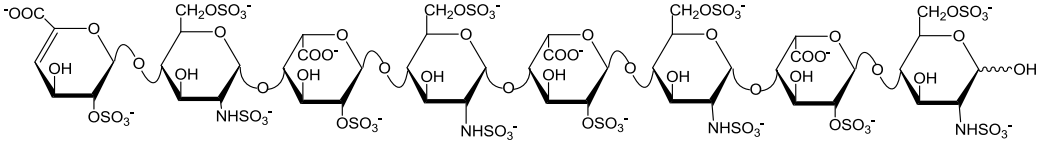

Figure 7. Heparan sulfate octasaccharide identified as an effective RSV binding glycan

(three sulfates per disaccharide) to enable a high affinity interaction with the RSV virion, the presence of three iduronates within the octasaccharide allowed for a high degree of conformational flexibility, permitting sampling of the best topologies for high affinity binding, and a simple procedure to isolate the octsaccaharide from bulk heparin material in sufficient amounts for structure/function studies was developed. The purification route, which is amenable to scale-up, is shown in **Figure 8**.

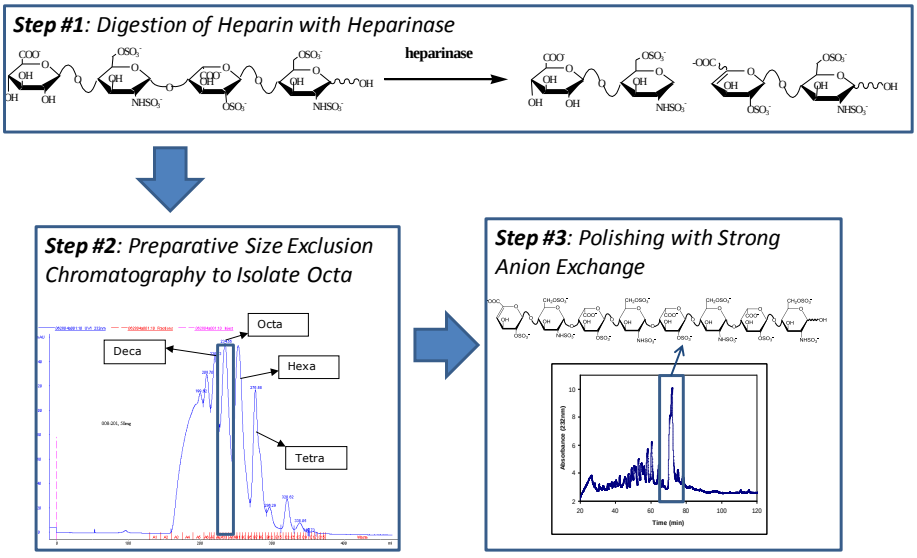

Figure 8: Purification scheme for the octasaccharide. Heparin is first digested with heparinase then material is size-fractionated and the octasaccharide pool is isolated. Finally, strong-anion exchange is used to isolate in mg amounts.

Optimal heparinase concentration and reaction conditions for digestion of heparin were chosen to yield significant amounts of octasaccharides (from ~30-50 mer). Since heparinase is a lyase, it cleaves the glycosidic linkage only at selected places (yielding even-numbered saccharide chains) and leaves behind a Δ4,5 double bond, a chemical signature that can readily be monitored at 232 nm. Using 232 nm monitoring, we then separated the oligosaccharide chains produced by size exclusion chromatography, and, after isolating the octasaccharide pool, polished the material using strong anion exchange. After desalting, multimilligram amounts of purified octasaccharide were obtained.

The purified heparan sulfate octasaccharide (HSocta) had strong anti-RSV properties when tested for its ability to block infection of MDCK cells (**Figure 9**). Full-length heparin sodium (the starting material) or purified HSocta was added to Vero cells simultaneously with RSV. Each material showed a significant ability to block RSV infection, with heparin sodium inhibiting >90% of PFU formation at a concentration of 1 µg/ml indicating that the native heparin displays surface glycans that very effectively bind RSV. The purified octasaccharide had less activity, blocking PFU formation roughly 50% at 1 µg/ml or higher. This was expected and is due to the inability of the purified material to form multivalent interactions with the RSV virion. Displaying HSocta on the surface of a liposome should recapitulate the multivalent binding while eliminating the anticoagulant and other detrimental effects of native heparin.

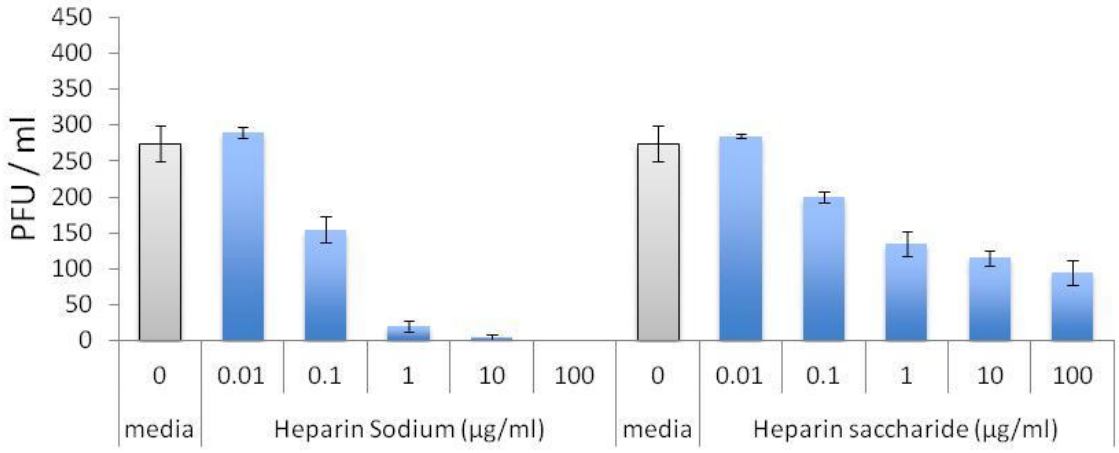

Figure 9. Efficacy of heparin sodium (left) and heparin sulfate octasaccharide purified by the described procedure (right) in clocking infection of MDCK by influenza PR/8.

Glycan chemistry design and incorporation strategy

Our approach to functionalizing the liposome surface has been to conjugate the viral glycan receptors to a linker then to a lipid anchor to create a glycolipid that could be incorporated into liposomes. Alternatives were to conjugate the carbohydrate to a different membrane-compatible molecule such as a protein in order to anchor it to the liposome surface, or to modify the surface of the liposome with the glycan after extrusion. The approach that we have taken has several advantages:

- the lipid backbone is much more stable during the extrusion process and during storage than a protein anchor
- the amount of glycan decorating the surface can be reproducibly adjusted by altering the amount in the extrusion

- the glycan and glycolipids can undergo independent QC prior to incorporation

The disadvantages of this approach are that the glycan must go through the extrusion process, which can affect its structure and stability. Also, using this method, the interior-facing surface of the liposome membrane will also express surface glycans though they are not available for binding. This may impact cost of production. Developing appropriate attachment chemistry and improving the glycolipid yield and purity turned out to be a major focus of the program.

LSTc glycolipid

In a standard sythesis, roughly 10 mg of purified LSTc is conjugated to the DOPE lipid anchor using the heterobifunctional linker N-(Fmoc-13-amino-4,7,10-trioxa-tridecyl)-succinamic acid. We use a two step process where the first step is attachment of the amine-linked unsaturated phospholipid, 1,2-Dioleoyl-sn-Glycero-3-Phosphoethanolamine (DOPE), to an Fmoc-protected linker acid using EDC as coupling reagent. The reaction product is purified by silica gel chromatography then the Fmoc deprotected to provide the amine for attachment with the free non-reducing sugar aldehyde of LSTc or LSTa via reductive beta elimination. This is described in **Figure 10**.

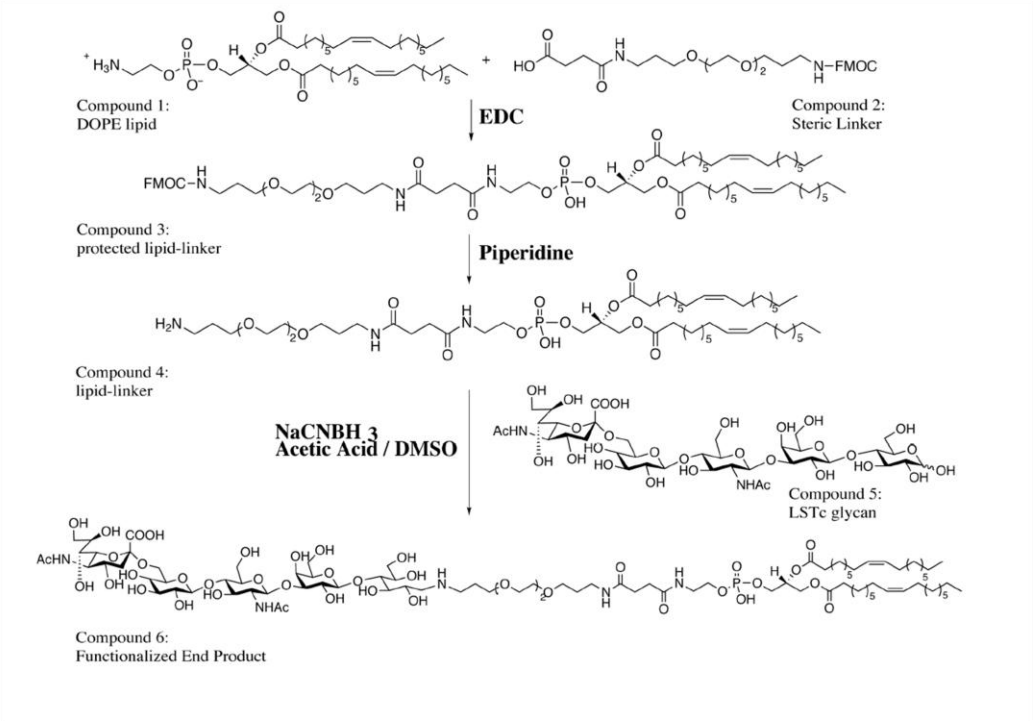

Figure 10. Scheme for reductive amination for conjugating glycan to an amine-functionalized lipid backbone.

After completion of the reaction the final product is (partially) purified using column chromatography. The partially purified product is the initially characterized by MALDI-MS spectroscopy to confirm the final glycolipid product, measured *m/z* value of 2033 Da (expected, 2034 Da). Standard column chromatography and HPLC are used to purify LSTa/c-DOPE, and product characterization is performed by NMR and MALDI-MS. Final glycolipid purity is typically greater than 90% and the reaction yield is 25-30%.

Heparan Sulfate glycolipid

Conjugation of HS oligosaccharide to DOPE was attempted using the reductive deamination reaction described above for generation of LSTc glycolipid but yielded no HS-oligosaccharide-DOPE product. This necessitated used of an alternate synthesis scheme and, after some exploration, amino-oxy derivatization was chosen as an option. The amino-oxy synthesis scheme is diagrammed in **Figure 11**. Unlike reductive amination, deprotected amino-oxy lipid inker was found to be unstable and could not be readily purified without the occurrence of significant side reactions. However, when the glycan was added to deprotected lipid-linker that was not purified (refer to the last two steps in **Figure 11**), the correct glycolipid product was recovered with high yield. Subsequently, the amino-oxy reaction was utilized to synthesize a pilot batch of HS-octasaccharide DOPE, which was the appropriate mass when analyzed using mass spectroscopy and had the appropriate structure when analyzed by NMR. The amino-oxy reaction was then successfully scaled up to yield 60 mg of high purity HS-octasaccharide-DOPE glycolipid.

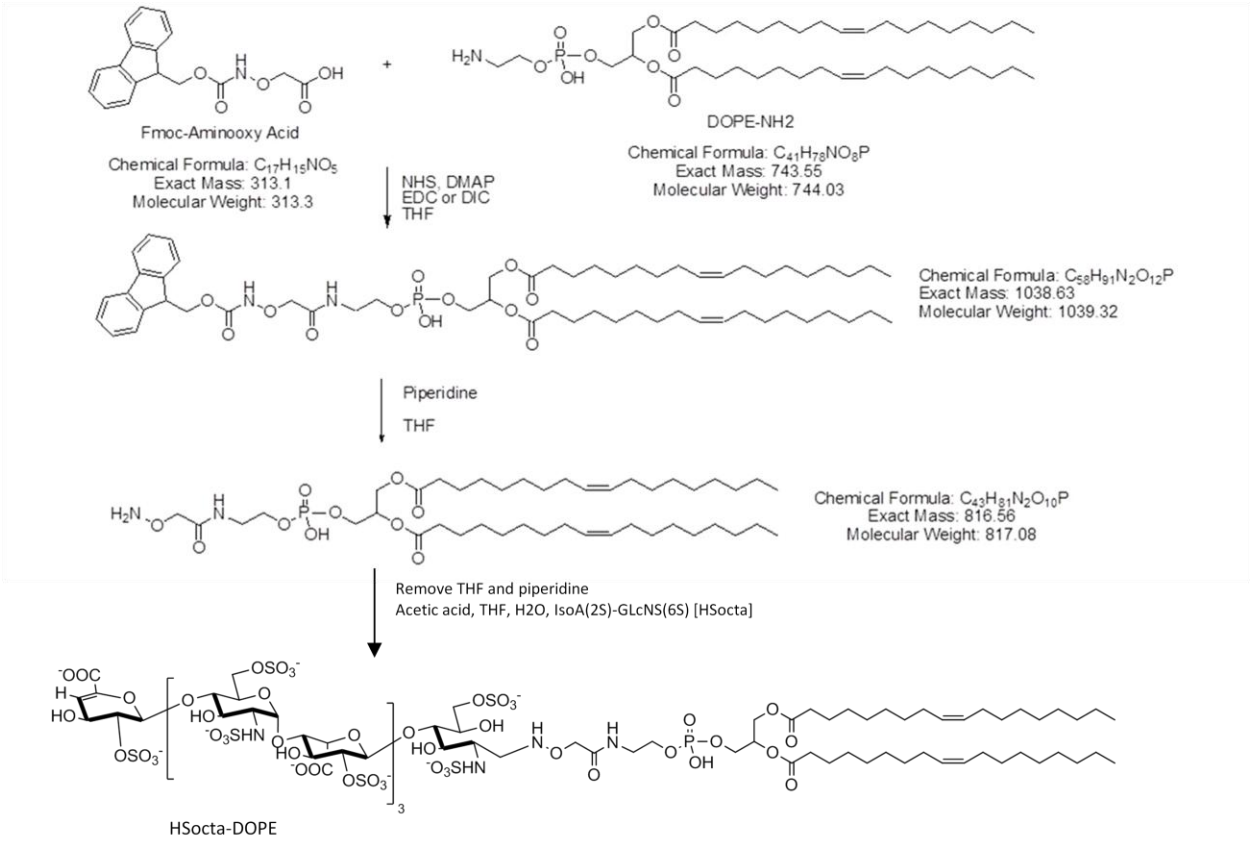

Figure 11. Amino-oxy synthesis scheme for linkage of HS-octasaccharide to DOPE.

Liposome Extrusion

DOPC (18:1 PC) was chosen as base lipid for liposome formulation since its long unsaturated hydrocarbon tail imbues a low gel transition temperature that causes relatively disordered membranes that remain fluid to be formed at room temperature (25˚C) or in the human body (37˚C). The lower transition temperature of DOPC also allows liposome to be manufactured without elevated temperatures. PC-based liposomes have also been used *in vivo* without encountering significant safety issues. As mentioned above, DOPE (18:1 PE) is used for glycolipid production since the viral glycan receptor can be conjugated via a readily-functionalized terminal amine. Also included in some liposome formulations is a small percentage of DOPE linked to the fluorescent

dye NBD that acts as a marker to assist with tracking and quantification. The related lipid DOPG (18:1 PG), which has a negatively-charged headgroup, was used to charge compensate for differing LSTc-DOPE percentages (the sialic acid on LSTc is negatively charged)(**Figure 12**). Liposomes were formulated using an extrusion technique derived from Hope, M. J. et al. 1985. (*Biochim. Biophys. Acta*. 812:55-65) typically using a 100 nm to 200 nm pore size.

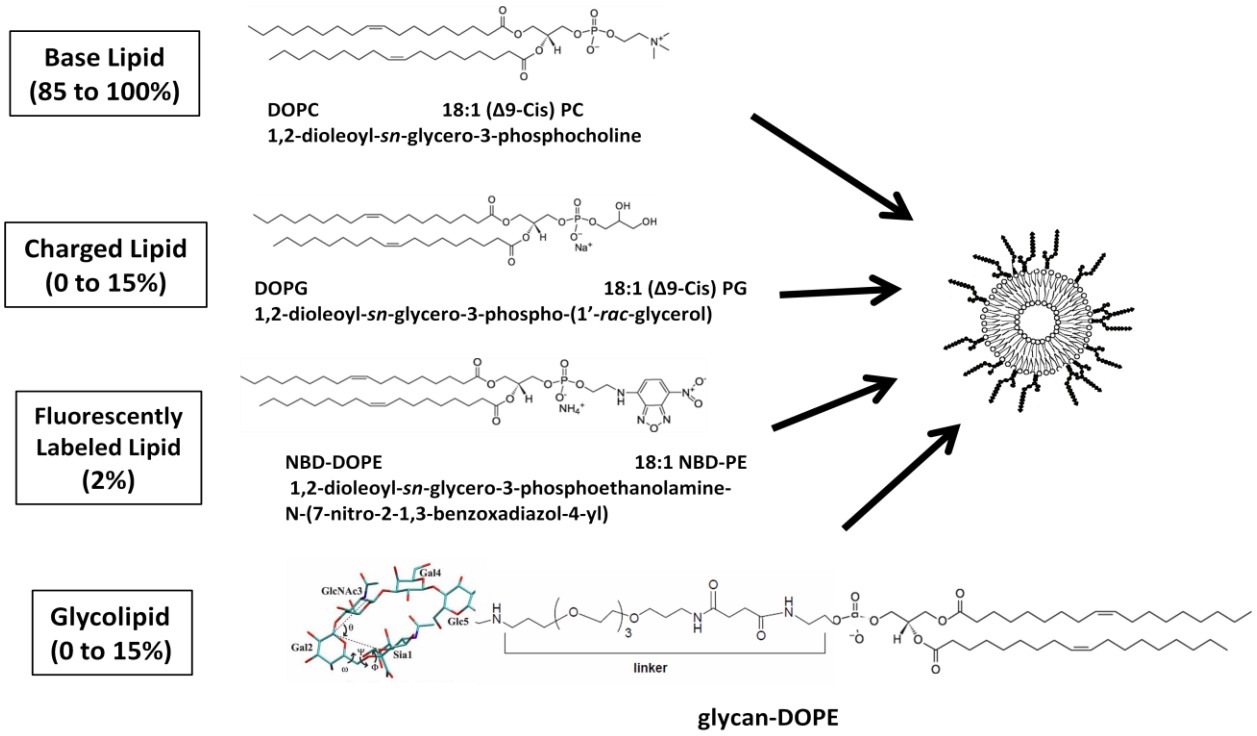

Figure 12. Lipids used in formulation of liposomes

Initial physical characterization of the bare liposomes was performed by dynamic light scattering (Malvern Instruments Zetasizer) to measure distribution of mean particle hydrodynamic size, polydispersity and zeta potential. The lipid content of each liposome batch was determined by colorimetric assay. Liposome stability was examined during shipping and storage, and results showed no significant changes to size or polydispersity upon shipping or long term storage at 4°C. Electron microscopy was also employed to assess the size and distribution of liposomes. An example of this is seen in **Figure 13**. Based on image analysis, these liposomes were 30 to 110 nm in diameter with an average diameter of 40.83 ± 14.80 nm. This is similar to the values obtained by DLS. It is unclear if the sample preparation or fixation procedures may have impacted the integrity of the liposomes.

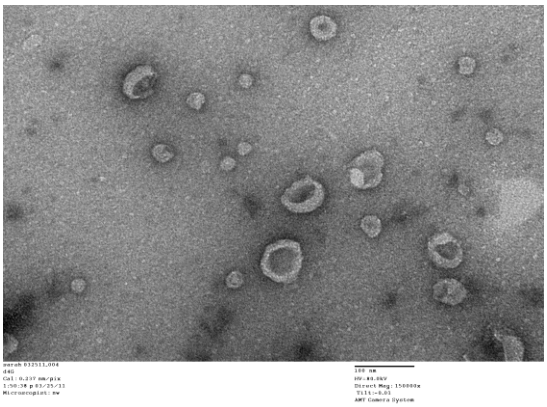

Figure 13. Scanning electron micrograph of LSTc-bearing liposomes. Visible are numerous collapsed liposome vesicles (expected with this fixation procedure) in the 30 to 110 nm size range. 100 nm scale bars are represented.

The concentration of active compound was expressed as either the concentration of glycan on the surface or the concentration of liposome particles. The concentration of surface glycan depends on the mol% of glycan-DOPE incorporated into the liposome and assumes 100% incorporation based on the empirically determined lipid concentration. Liposome particle concentration is calculated from the lipid concentration, the liposome diameter, and the average size of a lipid head group. Calculated liposome concentrations were verified by nanoparticle tracking using a Nanosight device.

Liposome production under GLP

Draper has implemented the synthesis of the glycolipids using good laboratory practice (GLP) in preparation for pre-IND studies. This required implementation of SOPs for processes involved in synthesis and for maintenance, calibration, and qualification of equipment involved in the production of glycolipid, and training of Draper staff on development and execution of SOPs. A GLP-compatible protocol for production of glycan-bearing liposomes was also developed. The protocol utilized by UCSB for glycan-bearing liposomes was sufficient to produce batches for research and development, but the process utilizes solvents not appropriate for use in humans and is also not scalable for making larger liposome quantities. Northern Lipids, a contract research organization that specializes in GLP/GMP production of liposomes, developed a new production process that circumvents these issues. Glycolipid was solublized in 25% H_2O/t-butanol then mixed with other lipids (DOPC and cholesterol) follows by lyophilization at -5˚C. The lipid mixture was then reconstituted in 300 mM sucrose, 10 mM histidine pH 6.5 then extruded with 5 passes through a 200 nm membrane at 400 psi. The use of t-butanol alleviates much of the solvent-related safety concerns and the production process is scalable to multiple liter batches at concentrations up to 100 mg/ml lipid. Pilot batches of liposomes produced by Northern Lipids using this process had the same physical properties as similar batches produced at UCSB and had nearly identical activity when compared in head-to-head in *in vitro* studies (data not shown). This demonstrated that the newly developed production process produced effective liposomes suitable for GLP/GMP scale-up and potential use in clinical trials.

Liposome aerosolization

Studies using a cascade impactor were performed to better understand the deposition of nebulized liposomes in the airway. Fluorescently-labeled liposomes lacking LSTc were produced in the manner described at a concentration of 1, 4, or 10 mg/ml, then aerosolized using an AeroNeb nebulizer connected to the cascade

impactor. Transit of liposomes through the device was determined by quantification of the fluorescent signal. As indicated in **Table 1**, the majority of the liposomes (51 to 64%) ended up in the fine particle fraction, which correlated to deposition in the alveoli. 18 to 23% of the liposomes were deposited in the upper airway, thought to be the most relevant site for blocking influenza infection, and 18 to 26% were in the inhalable fraction, which correlates to deposition in the nasal passages. With an increasing concentration of liposomes, a greater proportion was in larger droplets and should be deposited in the upper airway and nasal passages. This data indicates that it is possible to achieve 20 to 25% deposition of liposomes in the upper airway, which would be the desired target for prophylaxis.

Table 1. Distribution of deposition of aerosolized liposomes

Decoy Conc. (mg/ml lipid)	MMAD (µm)	Geometric std dev (µm)	FPF <5 µm	Upper Airway 5.3-14.1 µm	Inhalable > 14.1 µm
1	4.54	1.88	64 %	18 %	18%
4	4.94	1.99	62 %	14 %	24 %
10	5.96	2.26	51 %	23 %	26%

***In vitro* activity of LSTc-bearing liposomes**

Inhibition of HA binding to surface-bound glycans by LSTc-labeled liposomes

The glycan array was initially used to assess the ability of liposomes to block influenza HA from interacting with its receptor. This assay uses HA isolated from various influenza A strains and precomplexed with primary and secondary antibodies (resulting in four subunits locked together spatially) to more accurately represent the multimeric binding that occurs between influenza virions and cells. Results with precomplexed HA are reflective of natural binding as evidenced by the similar glycan binding specificity of precomplexed H1, H2, or H5 HAs to that of whole virions expressing the corresponding HA. To assess liposome efficacy, LSTa or LSTc attached to a surface was probed with pre-complexed HA from the influenza strain Alb58 or Viet04. Alb58 is of the H2 subtype and human-adapted so that it shows predominant binding to α2→6 linked SA like that of LSTc, while Viet04 is of the H5 subtype and preferentially binds to α2→3 linked SA like that of LSTa. In the absence of glycan-bearing liposomes, pre-complexed Alb58 HA bound well to LSTc but not to LSTa and pre-complexed Viet04 HA demonstrated a preference for binding to LSTa over LSTc (**Figure 14**). Alb58 HA binding to LSTc was nearly completely inhibited by 27.5 fmol LSTc-bearing liposomes, while binding of Viet04 to LSTa or to LSTc was unaffected. This indicated that LSTc-labeled liposome can block binding of HA from a human-adapted strain to an α2→6 linked SA but not HA from an avian-adapted strain to an α2→3 linked SA. Conversely, liposomes bearing 15 mol% LSTa were not able to inhibit the binding of Alb58 to LSTc and, surprisingly, were also only partially effective in competing with the interaction of Viet04 with LSTa on the array surface. This demonstrated that the LSTa-labeled liposomes had a lower affinity for influenza HA specific for α2→3 linked SA than LSTc liposomes do for HA specific for α2→6 linked SA. This was confirmed in subsequent assays examining the ability of glycan-bearing liposomes to block MDCK infectivity.

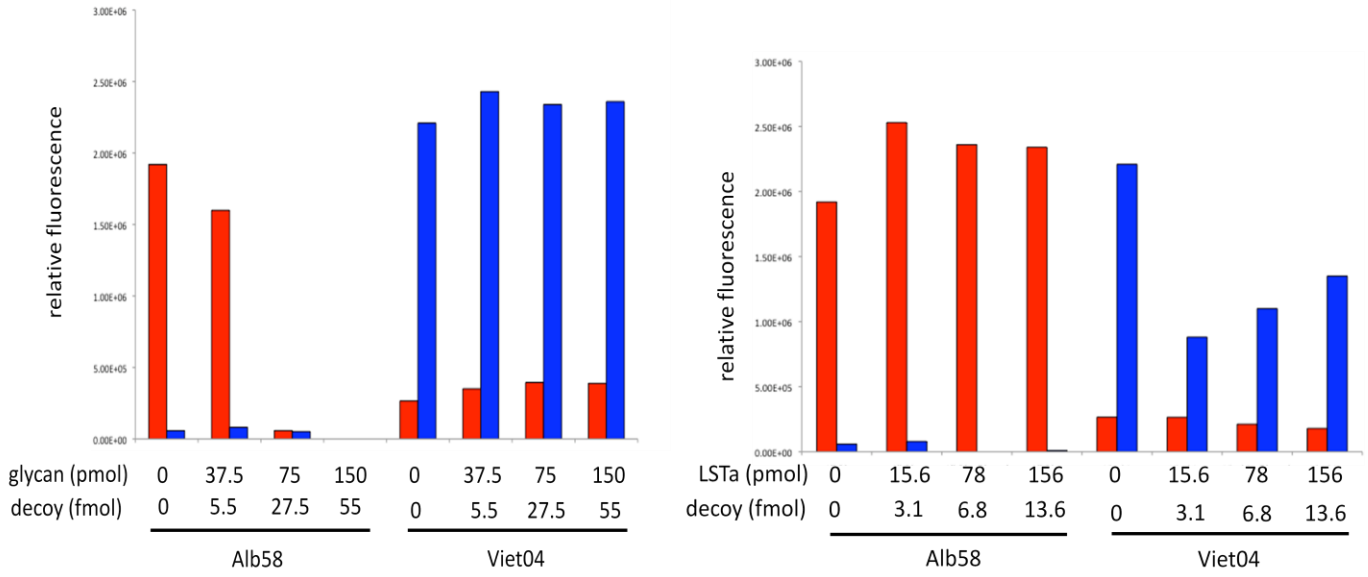

Figure14: Glycan array analysis of the effect of glycan-bearing liposomes on the binding of pre-complexed Alb58 or Viet04 HA to surface-bound LSTc (red) or LSTa (blue). Influenza HA was mixed with buffer only or the LSTc-labeled liposomes (15 mol% LSTc – left) or the LSTa-labeled liposomes (15 mol% LSTa - right) at the amount indicated, then bound to the glycan array.

Hemagglutination inhibition (HAI) assays

HAI was used as another screen of the anti-HA activity of different liposome batches since it can rapidly assess binding efficacy against different influenza A strains. Influenza A agglutinates RBCs to form a sheet and inhibition of this hemagglutination can be readily measured. Assessment of the HAI activity of LSTc- and LSTa-containing liposomes against range of influenza A strains showed that LSTc-containing liposomes inhibited the strains tested with a K_i^{HAI} in the nM range (**Table 2**). Soluble LSTc showed no inhibitory capability at >740 µM glycan, the maximum concentration tested, which showed that attachment of LSTc to the liposome surface resulted in more than a 1000-fold increase in binding activity. LSTa-containing liposomes were less effective at inhibiting hemagglutination than LSTc-containing liposomes and had no measureable inhibitory effect on the hemagglutination by human-adapted influenza A/Beijing. Additional data is summarized in our initial publication Hendricks et. al. (2013).

Table 2. HAI activity of leading liposome candidates vs different viral strains (K_i^{HAI} in nM glycan; nd= not determined)

glycan	mol%	PR8 (H1N1)	Philippines (H3N2)	Beijing (H1N1)	X-31 (H3N2)	Victoria (H3N2)	Hong Kong (H3N2)
LSTc	15	29	230	230	191	459	172
LSTa	30	228	911	>14,585	3247	2506	470

Improvement of liposome formulation for blocking infection of MDCK cells

The ability of liposomes to block influenza virus infection of Madin-Darby Canine Kidney (MDCK) cells grown in tissue culture was the primary *in vitro* assay used to assess efficacy of different formulations. MDCK cells express a variety of glycans with α2→3-linked and α2→6-linked sialic acid so can support the infection and

replication of a variety of influenza virus subtypes and strains. Glycan-bearing liposomes generally had no significant acute effect on the viability of MDCK cells, even at high concentration, when assayed using lactate dehydrogenase (LDH) release into the culture medium or other toxicity assays.

Over twenty different batches of LSTc-bearing liposomes, varying in formulations and/or production method, were produced and tested in MDCK cell infection assays. This series of experiments is summarized below:

- Inhibitory activity increased as the mol% of LSTc-glycolipid in the liposome formulation, and thus the amount of LSTc on the liposome surface, was increased from 0 to 7.5 mol% LSTc (Hendricks et al, 2013). Less total LSTc was required with LSTc-bearing liposomes with 7.5 mol% glycan compared to 5 or 1 mol% glycan, which indicated that liposomes with 7.5 mol% glycan were more effective. This was likely due to the improved multivalent interaction achieved by adding more LSTc to the liposome surface.
- LSTc-liposome inhibitory efficacy did not increase significantly when the LSTc concentration was increased beyond 7.5 mol%. Liposomes preparations with 15 or 30 mol% LSTc had roughly the same activity (**Figure 15**). This suggests a limit to the number of glycans that can be appropriately displayed from the glycan surface and/or interact with the influenza virion.

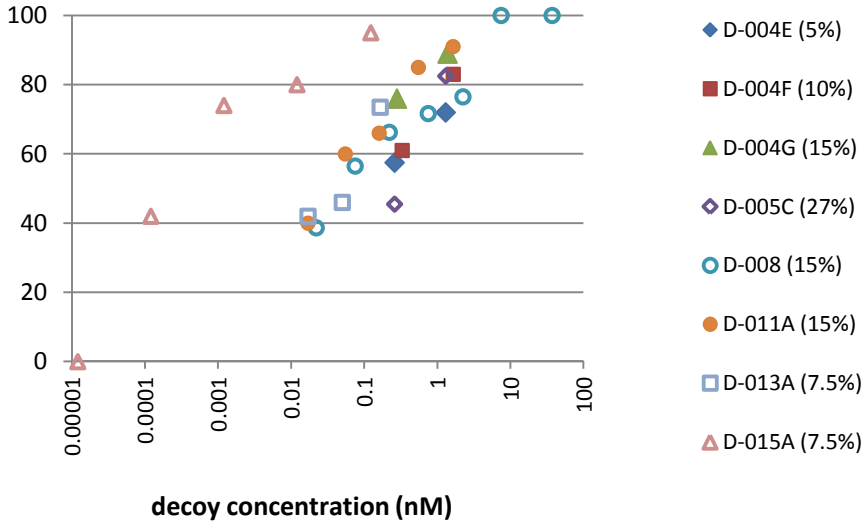

Figure 15: Comparison of *in vitro* activity of LSTc-bearing liposome batches. Various LSTc-bearing liposome batches containing 5, 7.5, 15, or 27 mol% LSTc-DOPE were tested for their ability to inhibit PR/8 infection of MDCK cells.

- When different extrusion membranes were utilized it became apparent that larger liposomes (100 to 130 nm diameter) have increased activity over their smaller (60 to 80 nm diameter) counterparts.
- The inclusion of 30% cholesterol improved the ability of liposomes to inhibit influenza infection, particularly with PR/8.
- Additional negative surface charge slightly increased liposome in a strain-specific manner.
- The inclusion of 10 mol% PEG-1000 reduced liposome efficacy in the formulations tested.
- LSTc-bearing liposome batches were more effective inhibiting PR/8 (H1N1) *in vitro* than Philippines X-79 (H3N2). This is shown with several liposome batches in **Figure 16**. The *in vitro* IC_{50} 0.5 pM liposome/1.2 nM LSTc for PR/8 and 4 pM liposome/30 nM LSTc for Philippines X-79.

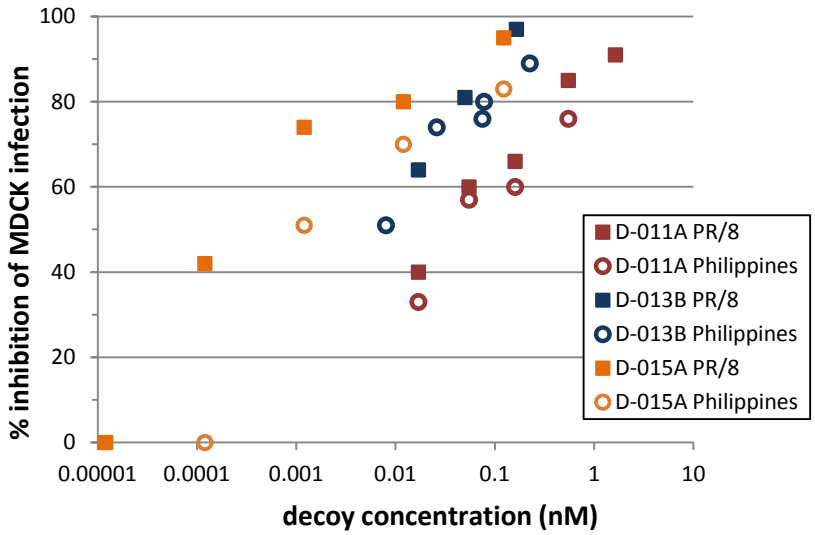

Figure 16. Comparison of LSTc-labeled liposomes vs. PR/8 (H1N1) and Philippines X-79 (H3N2). *In vitro* efficacy against PR/8 was greater than that against the Philippines strain.

Based on these results, a formulation consisting of 7.5 mol% LSTc-DOPE, 30% cholesterol, 62.5% DOPC with extrusion through a 200 nm membrane to produce liposomes in the 100 to 150 nm range was the process used to produce LSTc-labeled liposomes.

LSTc-labeled liposomes produced by this method were tested for their ability to prevent the cytopathic effects (CPE) of influenza virus on MDCK cells (**Figure 17**). LSTc-bearing liposomes and influenza virus were left in contact with cells for 48 hours and the amount of cytotoxicity was then assessed. The concentration of LSTc-labeled liposomes that achieved 50% inhibition of CPE (IC_{50}) depended on the amount of PR/8 viral challenge, with IC_{50}s of 10 nM with 0.1 MOI, 1.5 nM with 0.01 MOI, and 0.02 nM with 0.001 MOI. In a control experiment, liposomes lacking LSTc had no effect on CPE. This demonstrated that LSTc-labeled liposomes had long lasting ability to block influenza virus and protect cells from infection.

Using this same assay, LSTc-labeled liposomes were demonstrated to inhibit cell death caused by a range of H1N1 or H3N2 influenza strains, including human-adapted and pandemic (California/09 and San Diego/09) strains (**Table 3**). The ED50 ranged from 160 nm to roughly 1 µM LSTc, or 16 to 110 nM liposomes, depending on the strain. This confirmed that LSTc-liposomes had broad specificity in blocking influenza infection.

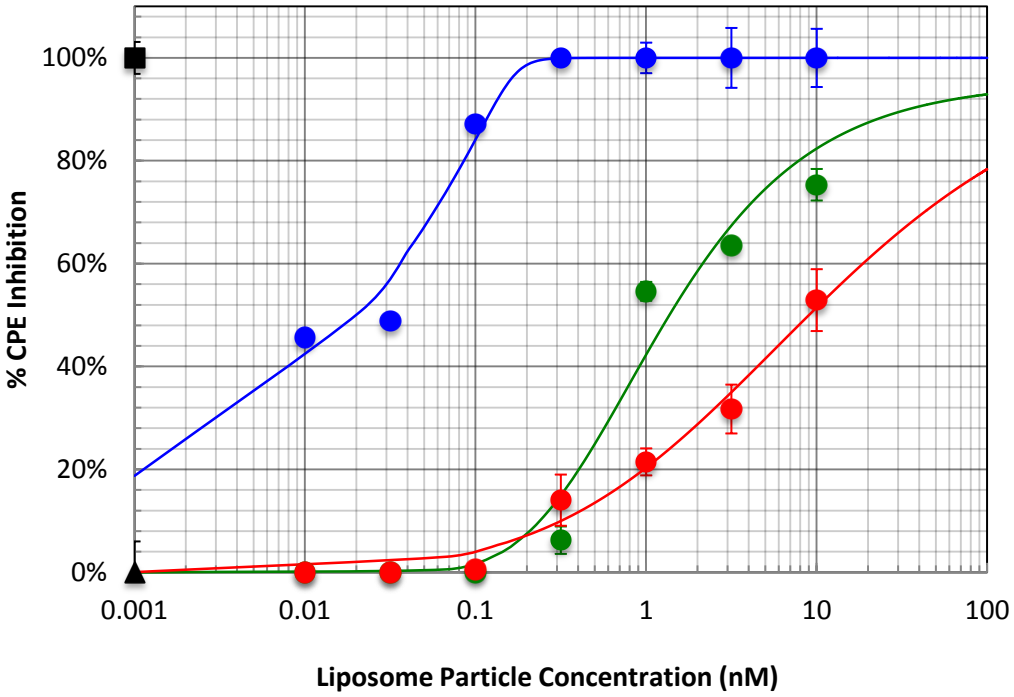

Figure 17. LSTc-bearing liposomes are able to block the cytopathic effect of influenza A. MDCK cells were treated with LSTc-labeled liposomes at the indicated concentrations then immedaitely infected with PR/8 influenza virus at an MOI of 0.001 (blue), 0.01 (green), or 0.1 (red). After 48 hours the amount of cell viability was determined with alamar blue. Cells receiving virus and liposomes lacking LSTc served as a control (black triangle), as did a well the received liposomes but no virus (black square).

Table 3. Inhibition of cell toxicity caused by H1N1 and H3N2 influenza strains

		ED50 (μM LSTc)	ED50 (pM liposome)
H1N1	A/Beijing/262/95	1.05	109.8
	A/Brisbane/59/2007	0.48	50.5
	A/California/04/2009	0.22	23.4
	A/PuertoRico/8/1934	0.21	22.0
	A/SanDiego/1/2009	0.16	16.3
H3N2	A/Aichi/2/68	0.76	79.1
	A/Brisbane/10/2007	0.45	46.9
	A/HongKong/8/68	0.73	76.2
	A/Sydney/5/97	0.73	75.6

The CC_{50} of LSTc-bearing liposomes for MDCK or primary airway epithelial cells, determined using alamar blue staining, was >75 µM LSTc. This yields a selectivity index (CC50/ED50) of ≥ 75 for LSTc-bearing liposomes, which is an initial indication that treatment is well-tolerated. Additional data demonstrating the ability of LSTc-labeled liposomes to reduce viral propagation and yield is published in Hendricks et al. (2013).

LSTc-bearing liposomes were also shown to block influenza infection of primary human bronchial epithelial (normal human bronchial epithelium or NHBE) cells, which are more representative of the type of airway cells encountered during infection. These commercially-available NHBE cells differentiate into representative airway epithelia when incubated in an air-liquid interface, i.e. with the basolateral surface bathed in medium and the apical surface exposed to air, and display different sialyated receptors than MDCK cells. PR/8 was able to effectively infect and propagate within these cells and, as monitored by the FFA assay, and LSTc-labeled liposomes were able to effectively block PR/8 infection and propagation in a concentration-dependent fashion (**Figure 18**). 3 nM LSTc-labeled liposomes reduced the fluorescent signal produced by influenza nucleoprotein by 70% relative to control liposomes lacking LSTc. The concentration of LSTc-bearing liposomes was roughly 100-fold greater than that needed to block influenza propagation in MDCK cells.

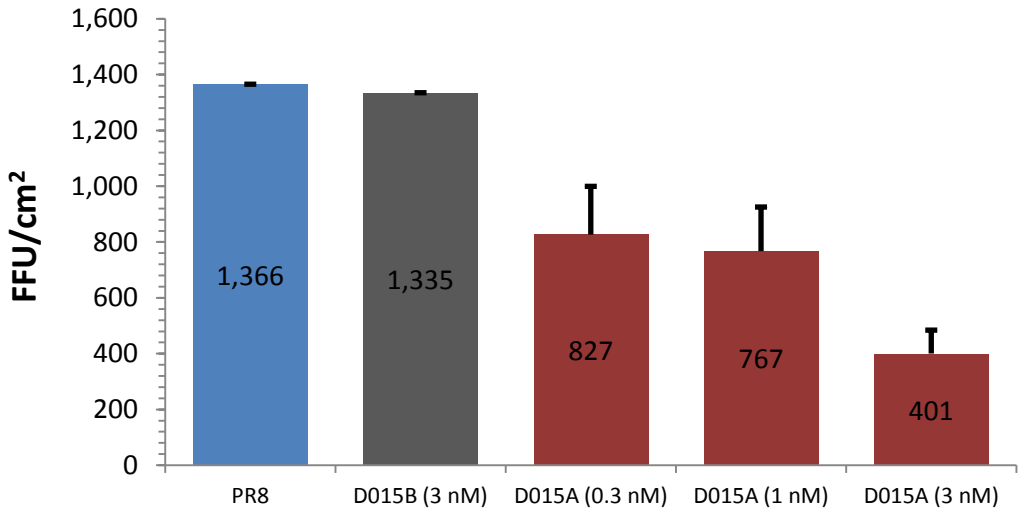

Figure 18. Efficacy of LSTc-bearing liposomes in inhibiting PR/8 infection of primary human bronchial cells (NHBE). Liposomes with 7.5 mol% LSTc (red) or those lacking LSTc (gray) were added to NHBE cell monolayers immediately prior to the addition of PR/8. A PR/8 infection lacking liposome treatment (blue) served as a control.

In vivo activity of current LSTc-bearing liposome formulations

We performed a number of independent studies that indicated LSTc-labeled liposomes, when mixed with virus prior to instillation, inhibit influenza PR/8 in the mouse model of infection. A summary of three replicate experiments was published in Hendricks et al. (2013) and is presented in **Figure 19**. Mice that received LSTc-bearing liposomes had a 33% increase of mean survival time post-infection compared to mice that received liposomes lacking LSTc. LSTc-bearing liposomes at the same dose that demonstrated efficacy when pre-mixed with virus prior to infection were not effective when given one hour prior to influenza infection. Since *in vitro* data suggests that liposomes are stable for at least 4 hours in up to 50% serum (data not shown), the lack of efficacy of prophylactic treatment in the mouse model is likely due to liposomes being transported by mucus

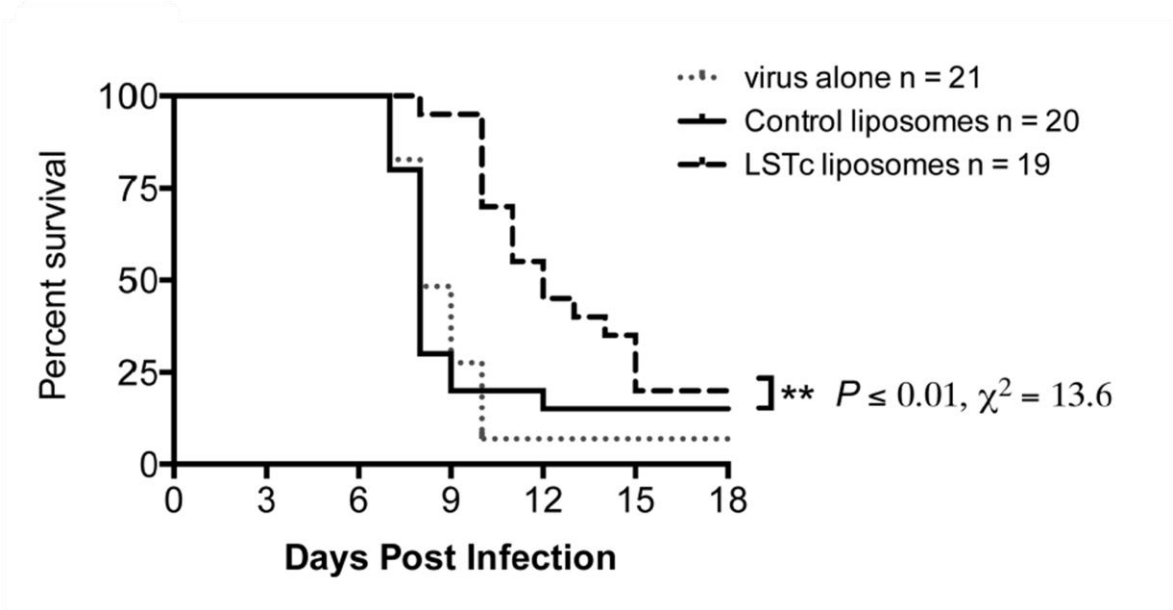

Figure 19. LSTc-liposomes extend survival following a lethal influenza A challenge. A single dose of LSTc-bearing liposomes premixed with an LD_{95} of PR/8 (H1N1) increases mouse longevity and survival. Liposomes with 7.5 mol% LSTc (dashed line) or without LSTc (solid line) were pre-mixed with 1,000 PFU for 30 minutes the instilled intratracheally into C57BL/6 mice. Mice were monitored daily. The survival advantage from a single dose was statistically significant ($\chi 2$ = 13.6, $P \leq 0.01$; n ≥ 19 for each arm).

and/or diluted after installation so that they were not at sufficient concentration to inhibit the newly-instilled virus. LSTc-bearing liposomes also did not demonstrate significant efficacy in limiting infection from a lethal dose of Philippines X-79 (H3N2), despite having significant *in vitro* activity against this strain (**Figure 20**). Due to inter-strain differences, a higher dose of Philippines X-79 (at least 7,000 PFU vs. 1,000 PFU of PR/8) is needed to achieve an LD_{95} via orotracheal instillation in the mouse model.

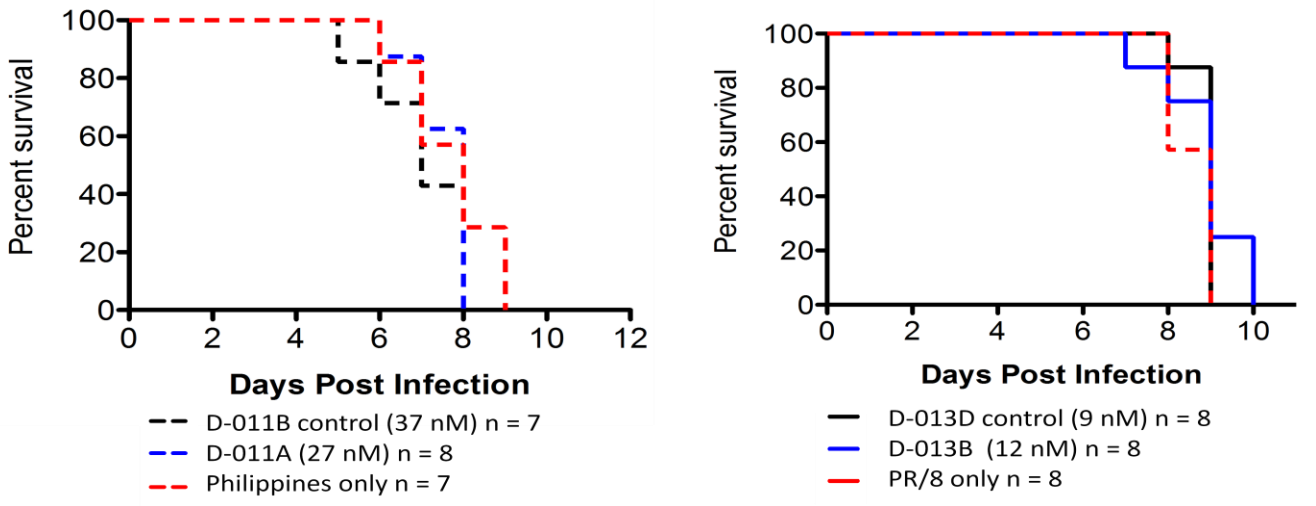

Figure 20: LSTc-liposomes pre-mixed with Philippines X-79 do not block infection in mice. A single dose of LSTc-bearing liposomes premixed with an LD_{95} of Philippines X-79 (H3N2) had no effect on mouse longevity or survival. Two different batches of liposomes with (D-011A of D-013B) or without (D-011B or D-013D) LSTc were mixed with 20,000 PFU (left) or 7,000 PFU (right) of Philippines X-79 for 30 minutes at 37˚C then administered to mice via orotracheal instillation.

Since the likely mechanism of action of the liposomes is direct competitive inhibition, we would anticipate a 7-fold higher dose of liposomes is required to inhibit infection by the Philippines X-79 strain. This can be achieved by either increasing the liposomes dose or by giving daily or twice daily doses.

Pharmacokinetics of LSTc-bearing liposomes

The *in vivo* fate of LSTc-bearing liposomes was assessed in pharmacokinetic studies where radiolabeled liposomes were instilled into the respiratory tract of mice. Initial studies were performed with liposomes lacking LSTc (62.5 mol% DOPC, 30 mol% cholesterol, and 7.5 mol% DOPG) and labeled with ^{3}H-cholesterol hexadecyl ether (0.05 µCi/mouse), which incorporates into the liposomal membrane, and ^{14}C-sucrose (0.05 µCi/mouse), which was encapsulated. Using liposome preparations of 10 or 100 mg/ml lipid, equivalent to 25 or 250 mg/kg, a significant proportion of the ^{3}H-cholesterol hexadecyl ether remained in the lungs of mice for the 72 hour duration of the experiment (**Figure 21**). This indicated that lipids present in the delivered liposomes remain in the airway of mice for at least several days. Conversely, over 90% of the ^{14}C-sucrose was eliminated by 24 hours, which suggested that the liposome contents are retained in the mouse airway for a much shorter period. Possible explanations for the difference between the fate of the labeled substances could be that the liposomes were disrupted or that they become "leaky" to small molecules such as sucrose when exposed to protein and lipid surfactants in the airway. The pharmacokinetic profile was not dependent on the liposome concentration.

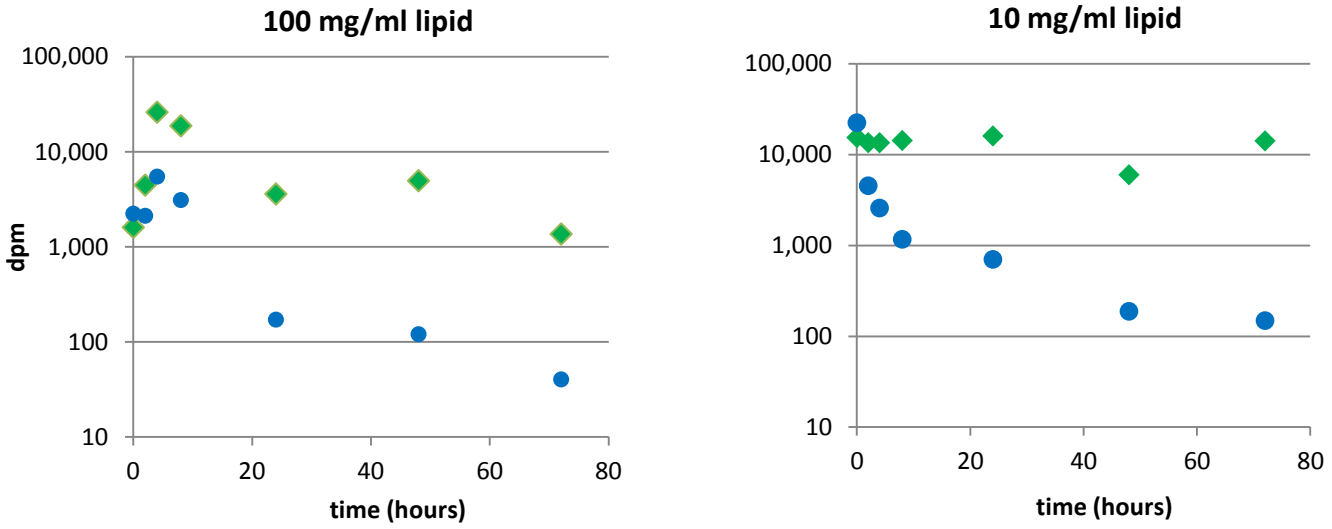

Figure 21. **Pharmacokinetic profiles of liposomes lacking LSTc in the lungs of mice**. Balb/c mice were given a 50 µl dose of 100 mg/ml or 10 mg/ml liposomes labeled with 0.05 µCi ^{3}H-cholesterol hexadecyl ether and 0.05 µCi ^{14}C-sucrose. At the times indicated, mice were sacrificed and the dpm present in lung tissue was determined. Each point represents the average of 5 mice.

The *in vivo* fate of liposomes labeled with 7.5 mol% LSTc was determined in a similar manner but without the encapsulatation of ^{14}C-sucrose since results using that isotope were largely uninformative. In the lungs of mice sacrificed immediately after instillation of the ^{3}H-labeled LSTc-bearing liposomes, only 37% of the radioactivity was recovered, which indicated significant losses to the nasal passages, esophagus, or elsewhere (**Figure 22**). Of the radiolabel that entered the lungs, its disappearance is biphasic with 30% of the recoverable ^{3}H-labeled cholesterol being eliminated from the lungs linearly over 3 days and 70% of the recoverable ^{3}H-labeled

cholesterol remaining associated with the lungs for 14 days or more. Our presumption is that the first phase represents the fate of intact liposomes and that these have a $t_{1/2}$ of roughly 1.5 d. The second phase represents cholesterol that is dissociated from liposomes and incorporated into lung tissue so that it remains in the lung for 2 weeks or more. However, the integrity of the liposomes cannot be determined and future studies will be designed to evaluate the PK of intact liposomes and their correlation to anti-viral activity.

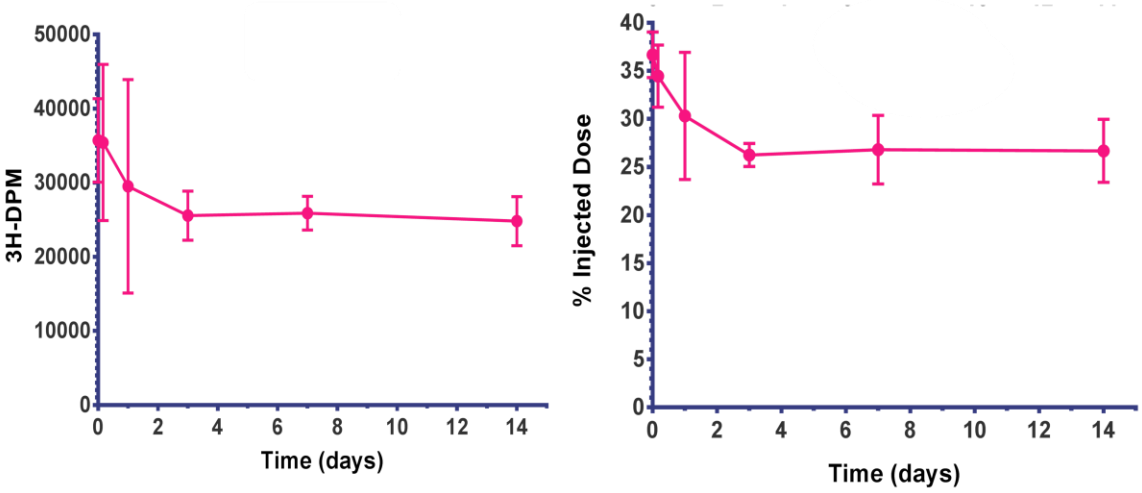

Figure 22. **Pharmacokinetic profile of LSTc-labeled liposomes in the lungs of mice**. Balb/c mice were given a 50 µl dose of 10 mg/ml LSTc-labeled liposomes labeled with 0.05 µCi ^{3}H-cholesterol hexadecyl ether. At the times indicated, mice were sacrificed and the dpm present in lung tissue was determined. The data is expressed as total dpm recovered (left) or as a percentage of the initial dose (right). Each point represents the average of 8 mice.

LSTa-labeled liposomes

Liposomes containing 30mol% LSTa were over 10-fold less effective than similar LSTc-labeled liposomes against the mouse-adapted PR/8 (H1N1) strain and at least 4-fold less effective than LSTc-labeled liposomes against Philippines (H3N2) strain (**Table 1**). Additional experiments demonstrated that liposomes with 7.5 mol% or 15 mol% LSTa inhibited the H1N1 and H3N2 strains but at a 100-fold higher concentration than LSTc-labeled liposome for PR/8 (11.7 nM vs. 50 pM) and at over a 30-fold greater concentration than that needed to block Philippines X79 (15.5 nM vs. 390 pM). Clearly, the LSTa-labeled liposomes were less effective than LSTc-labeled liposomes in interacting with mouse-adapted strains and blocking infection *in vitro*. This was possibly due to the HA binding specificity of the particular mouse-adapted strains used or due to differences in the presentation of LSTa and LSTc on the liposome surface.

We examined if the two liposome types could act synergistically to block influenza infectivity. Different amounts of LSTc-labeled liposomes (15 mol% LSTc) were combined with various amounts of LSTa-labeled liposomes (15.5 mol% LSTa), then were mixed with either PR/8 or Philippines and assayed for their ability to block MDCK infectivity. The efficacy of LSTa-labeled liposomes or LSTc-labeled liposomes alone versus PR/8 was similar to that seen in other experiments. There appeared to be a slight improvement in the activity of LSTc-bearing liposomes in the presence of LSTa-labeled liposomes that did not elicit an effect alone (93 pM or 310 pM – **Figure 23**), but no synergistic effect was seen when the experiment was repeated with the Philippines (H3N2) strain. This suggested that any possible synergistic effect of the two liposome types is strain or subtype specific, and a mixture of LSTa- and LSTc-bearing liposomes provided no advantage over LSTc-

labeled liposomes alone. Also, since LSTc-bearing liposomes alone were highly effective in blocking the mouse-adapted H1N1 and H3N2 influenza strains and LSTc is most relevant glycan for blocking infection by human-adapted influenza A strains (due to their reliance on α2→6 sialylated, umbrella-like glycan receptors), a programmatic decision was made to focus solely on optimization, testing, and development of liposomes bearing LSTc with no further research on LSTa-bearing liposomes.

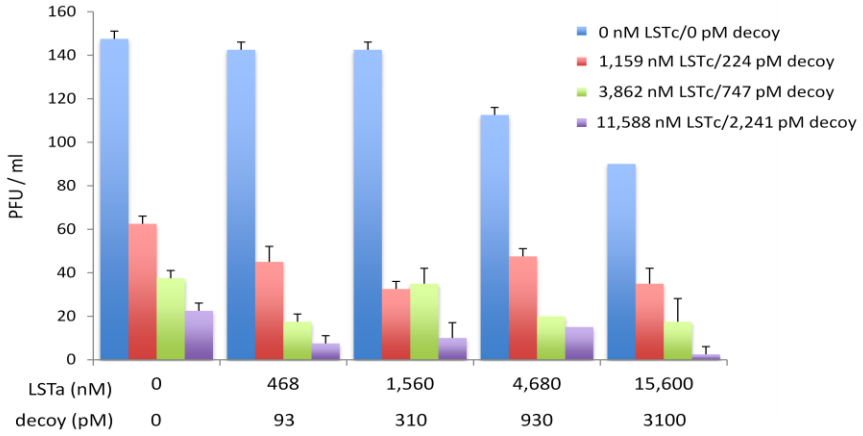

Figure 23: *In vitro* efficacy of combinations of LSTc- (15 mol% LSTc) and LSTa-labeled (15 mol% LSTa) liposomes against PR/8. Liposomes at the concentrations indicated were mixed with virus then added to MDCK cells. Error bars represent standard deviation from the mean of triplicate samples.

Mechanism of action of LSTc-bearing liposomes

To support our hypothesis that the mechanism of action of the LSTc-labeled liposomes was through binding to the virus, transmission electron microscopy was used to assess the interaction of LSTc-bearing liposomes and influenza PR/8. Roughly 10^9 LSTc-labeled liposomes diluted in PBS were mixed with 10^5 PFU of PR/8 then added to carbon-coated grids for imaging. LSTc-bearing liposomes bind to and accumulate around the virus particles, while control liposomes lacking LSTc do so to a significantly lesser extent (**Figure 24**). This indicated that LSTc on the liposome surface initiates interaction with the virus. In these images, the liposomes appear fairly heterogeneous in size, which may be due to a result of the preparation procedure.

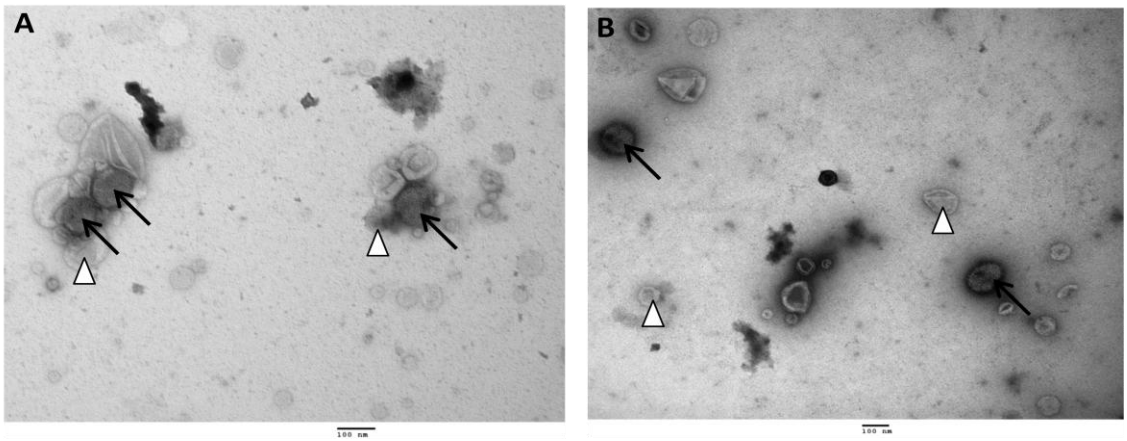

Figure 24: Transmission electron microscopy of liposome-virus interactions. $1x10^9$ 7.5 mol% LSTc-labeled liposomes (image A) or liposomes lacking LSTc (image B) mixed with roughly $1x10^5$ PFU of PR/8 then immediately bound onto grids for imaging. Virus particles (black arrows) maintain their shape, stain more darkly, and have a textured appearance. Liposomes (white arrowheads) collapse during dehydration and do not keep their spherical shape.

To further study anti-influenza liposome mechanism of action, we compared the efficacy of LSTc-labeled liposomes added prior to, during, and after infection of MDCK cells with PR/8 (H1N1). More efficacy was achieved when the LSTc-labeled liposomes and virus were pre-mixed for 30 minutes prior to infection, which inhibited viral yield roughly 80% (**Figure 25**). Adding LSTc-labeled liposomes to the MDCK cells immediately prior to influenza virus also caused a significant reduction in infection of approximately 70%, not statistically different than pre-mixing liposomes and virus. Prophylactic addition of the LSTc-labeled liposomes to the cells 1 hour prior to viral infection reduced their ability to inhibit infection, with viral yield blocked 50%. When LSTc-labeled liposomes were added 1 hour after infection, they had no ability to reduce viral propagation. These results are consistent with LSTc-bearing liposomes interfering with the binding of influenza HA to receptors on the MDCK cell surface. The liposomes perform best when given an opportunity to bind virions prior to infection but are ineffective once influenza has an opportunity to interact with cells.

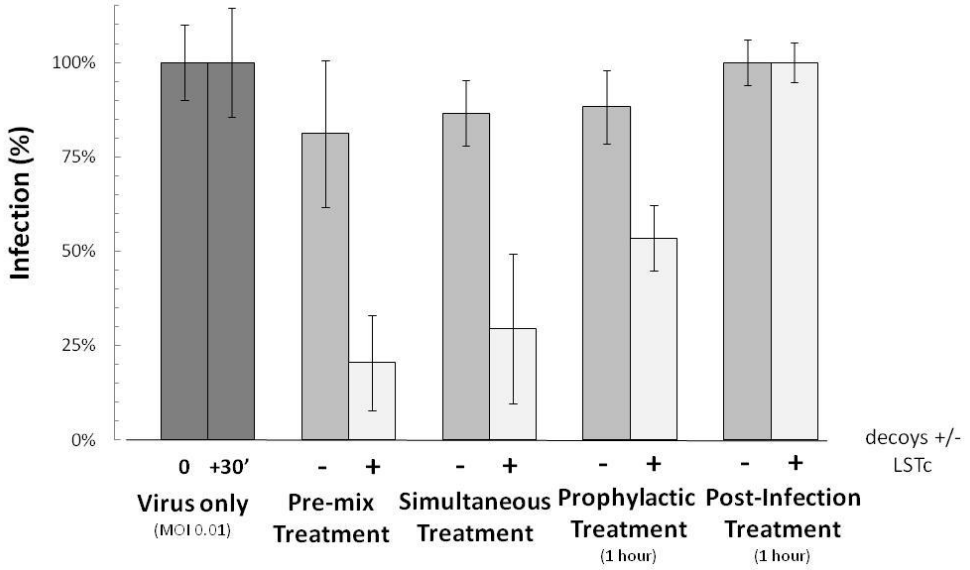

Figure 25. *In vitro* efficacy of LSTc-bearing liposomes added at various times relative to infection. Liposomes with (light grey) or without (dark grey) LSTc were added to MDCK cells immediately before (simultaneous treatment), 1 hour before (prophylactic treatment), or one hour after infection with 0.01 MOI of PR/8. As a control, liposomes were premixed with virus for 30 minutes at 37˚C then the mixture was added to MDCK cells (pre-mix).

To further study the efficacy of LSTc-labeled liposomes added prophylactically, LSTc-labeled liposomes were added to MDCK cells 2 to 6 hours prior to infection with PR/8. Compared to liposomes lacking LSTc, LSTc-bearing liposomes caused a 41 to 66% reduction in infection when added 2 to 6 hours prior to virus (**Figure 26**). When LSTc-labeled liposomes were pre-mixed with PR/8, infection was reduced 86% in this assay. So, while prophylactic addition of liposomes was not as effective as pre-mixing, liposomes were still effective when added up to 6 hours prior to virus infection. This indicated that the liposomes are stable in tissue culture for many hours and demonstrated stability under physiologic conditions. These results confirmed what was seen in PK studies.

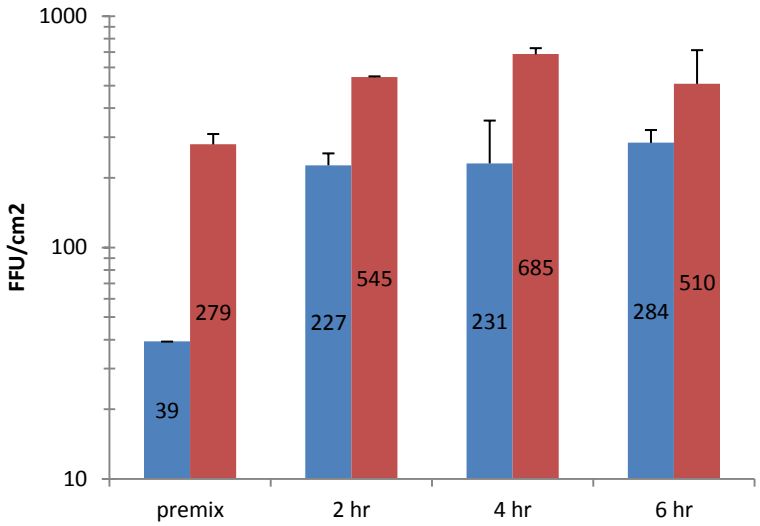

Figure 26. Prophylactic *in vitro* efficacy of LSTc-bearing liposomes. Liposomes with (blue) or without (red) LSTc were added to MDCK cells 2, 4, or 6 hours prior to infection with PR/8. As a control, liposomes were premixed with virus for 30 minutes at 37˚C. Influenza virus loses infectivity when stored at 37˚C, so the pre-mixed control has reduced fluorescence relative to the other controls.

Binding comparisons of liposome formulations using surface plasmon resonance

Surface plasmon resonance (SPR) imaging detects the presence of an analyte on a chemically modified gold surface by the change in local index of refraction that occurs upon adsorption. The SPR signal is a measure of mass concentration at the sensor chip surface, allowing analyte and ligand association and dissociation to be observed. From these observations, rate constants as well as equilibrium constants can be calculated. Using SPR, we assessed the affinity of LSTc-labeled liposomes for HA from human-adapted influenza A/New Caledonia/20/99 (H1N1). The HA from this strain, similar to that of other human-adapted strains, preferentially binds to glycans like LSTc that terminate in α2→6 linked SA and adopt an umbrella conformation. 7.5 mol% LSTc-bearing liposomes were shown to interact with HA purified from IFA H3N2 with a K_d of 580 pM, which represents high affinity binding similar to effective anti-influenza antibodies (**Figure 27**). Liposomes lacking LSTc showed no binding to New Caledonia/99 HA. This demonstrated that LSTc-liposomes have good binding affinity toward influenza HA and an on and off rate that should promote liposome-viral interaction.

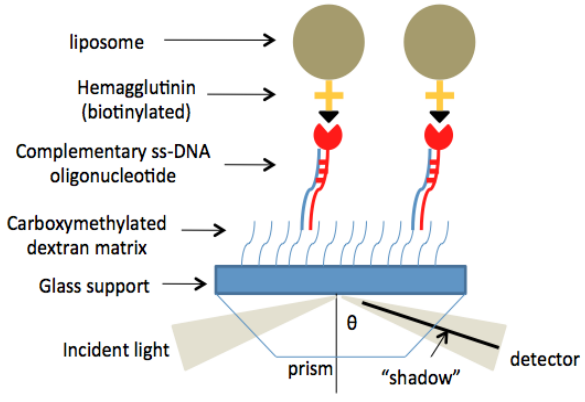

batch	k_a (1/Ms)	k_d (1/s)	K_d (nM)
1	$3.3\text{x}10^{7} \pm 9.6\text{x}10^{4}$	$1.9\text{x}10^{-3} \pm 4.3\text{x}10^{-6}$	0.58
2	$3.8\text{x}10^{7} \pm 2.0\text{x}10^{5}$	$1.2\text{x}10^{-3} \pm 8.6\text{x}10^{-6}$	0.32

Figure 27. Diagram of method used to measure binding affinity of LSTc-labeled liposomes to influenza HA (left) and calculated on-rate (k_f), off-rate (k_b), standard error (SE), and dissociation constant (K_d) of the binding of two different batches of 7.5 mol% LSTc-bearing liposomes to HA from human-adapted influenza A/New Caledonia/20/99 (H1N1 – right).

To further examine the interaction of influenza A virus (IAV) and LSTc-bearing liposomes in the context of mammalian cells, the Ploegh lab at the Whitehead Institute provided viral particles (WSN HA-647) that could be enzymatically labeled with a fluorophore. In an experiment performed at UMass Medical School, three different doses of these labeled virions were added to human alveolar basal epithelial cells (A549 cells) in the presence of LSTc-bearing liposomes or control liposomes lacking LSTc. Binding of fluorescent virions to single cells was assessed by flow cytometry. WSN HA-647 in combination with control liposomes showed a high degree of binding to A549 cells (**Figure 28**), with no significant difference in A549 cells challenged with control liposomes mixed with 1.3, 6.5, or 13 HA units of WSN HA-647. However, liposomes bearing 7.5 mol% LSTc reduced viral binding when challenged with WSN HA-647. LSTc-bearing liposomes decreased 75%, 79% and 54% of binding when challenged with 1.3, 6.5, or 13 HA units of WSN HA-647. These results show that LSTc-bearing liposomes competitively bound to influenza, and are thus able to block its adhesion to SA on uninfected cells and limit infection. In summary, this series of experiments supports LSTc-bearing liposomes directly binding to influenza virions and inhibiting viral entry as the mechanism of action.

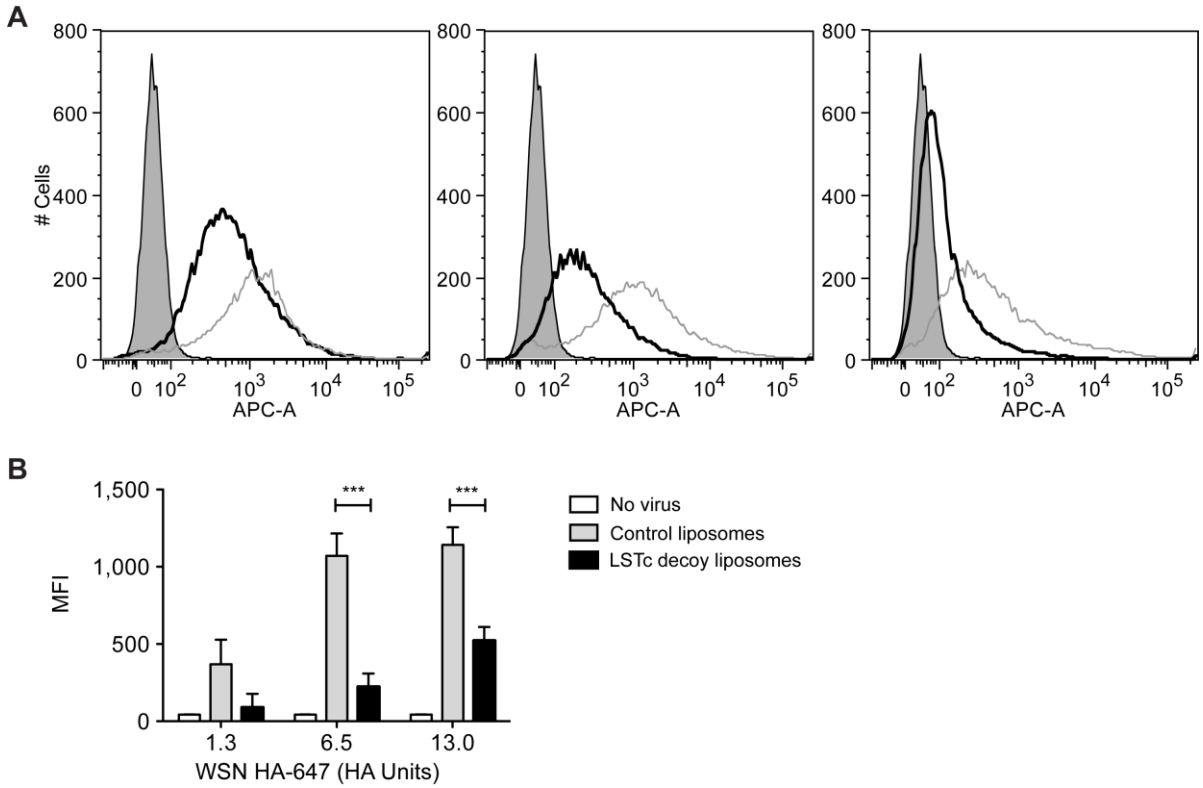

Figure 28. LSTc-containing liposomes inhibit binding of influenza A virus to A549 cells. A. Representative flow cytometry plots of A549 cells treated with 1.3 HA units (left), 6.5 HA units (middle), or 13 HA units (right) of fluorescently-labeled WSN HA-647 that was untreated (shaded), mixed with liposomes lacking LSTc (gray lines), or mixed with liposomes bearing 7.5 mol% LSTc (black lines). B. Mean fluorescence intensity of data in A. Error bars represent the standard error, *** indicates $P < 0.001$ for control vs. LSTc-bearing.

Efficacy of combinations of LSTc-labeled liposomes and influenza neuraminidase inhibitors

Influenza neuraminidase (NA) hydrolyzes the terminal sialic acid residues on newly formed virions and host cell receptors to help virus release from infected cells and spread within the respiratory tract. LSTc, like all influenza receptor glycans, contains a terminal sialic acid with the potential to be hydrolyzed by influenza NA, which would result in LSTc-labeled liposomes being rendered less effective. To see if inhibition of influenza NA enhanced LSTc-labeled liposome efficacy, liposomes were combined with two specific NA inhibitors, oseltamivir and zanamivir, each of which is FDA-approved for influenza therapy in humans. The NA inhibitors enhanced LSTc-labeled liposome anti-viral activity. Data for zanamivir is shown (**Figure 29**), and experiments with oseltamivir produced similar results. A single dose of 1 or 10 µM zanamivir mixed with influenza PR/8 and plain liposomes lacking LSTc did not have a significant effect on viral yield. However, this same zanamivir dose was able to enhance the inhibitory activity of LSTc-labeled liposomes when co-incubated with virus and liposomes. This indicated that inclusion of a NA inhibitor during virus-liposome interaction increased liposome efficacy. Therefore, sialic acid on the LSTc decorating the liposome surface appears to be hydrolyzed by influenza NA and this can diminish the inhibitory ability of liposomes.

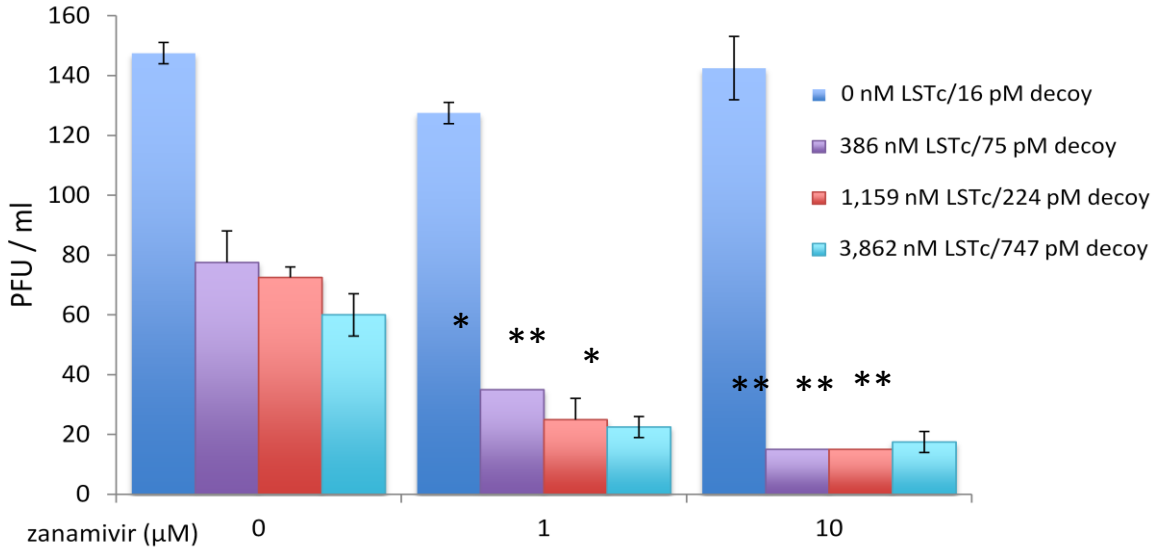

Figure 29: Effect of zanamivir on LSTc-labeled liposome inhibition of PR/8 infection of MDCK cells. Virus was mixed with liposomes lacking LSTc (blue bars) or LSTc-labeled liposomes at the concentrations indicated plus 0, 1, or 10 µM zanamivir. The reference values for statistical analysis are samples lacking NA inhibitor. * $p < 0.05$, ** $p < 0.01$

This hypothesis was then tested in a mouse model using PR/8. Because zanamivir has a short *in vivo* half-life, a single dose of zanamivir at the appropriate concentration should inhibit influenza NA in the short term but not significantly inhibit progression of influenza infection in the mouse. Pilot studies identified 0.01 mg/kg zanamivir the appropriate dose for a 1,000 PFU infectious dose of PR/8 (data not shown). To test the if NA inhibitor present during pre-mixing increased *in vivo* efficacy of LSTc-labeled liposomes, zanamivir was added to liposome/virus mixtures during their incubation period. As **Figure 30** illustrates, LSTc-labeled liposomes, both untreated and treated with zanamivir, had a significant effect on reducing mortality associated with infection by influenza PR/8. None of the mice treated with PR/8 only or PR/8 exposed to liposomes lacking LSTc survived after day 11 post-infection. However, mice treated with the LSTc-bearing liposomes D survived longer (until day 14) and had significantly less infection-associated mortality, with 3/8 mice surviving the

study, than mice receiving virus only or virus plus matching liposomes lacking LSTc (p = 0.005). 25 µM zanamivir alone slightly inhibited PR/8 infection, as 2/6 mice treated with a single dose of zanamivir survived (p = 0.007 vs. no treatment) and 1/8 mice receiving zanamivir plus liposomes lacking LSTc survived (p = 0.103 vs. liposomes lacking LSTc only).

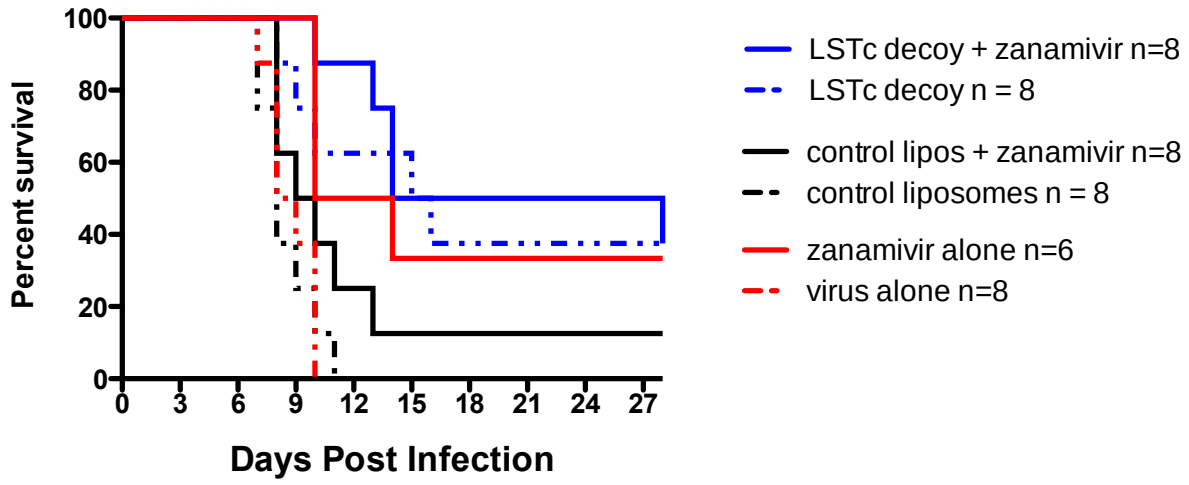

Figure 30: Prevention of mortality associated with PR/8 infection of the mouse by LSTc-bearing liposomes with or without zanamivir. 1,000 PFU of PR/8 was mixed with buffer (red), LSTc-labeled liposomes (blue; 171 µM LSTc/27.4 nM liposome) or liposomes lacking LSTc (black; 0 µM LSTc/36.7 nM liposome). One set of mixtures was untreated (dashed lines) while an identical set was mixed with 25 µM zanamivir (solid lines). All sets consisted of 8 mice with the exception of the arm that received 25 µM zanamivir alone, which had 6 mice. Mixtures were incubated for 30 min at 37˚C then delivered to mice via the orotracheal route.

There was no significant difference in the survival of mice receiving LSTc-labeled liposomes with or without zanamivir (p = 0.812). So while this study indicated that LSTc-labeled liposomes themselves are effective in increasing the length of survival and reducing mortality in mice infected with influenza virus, the effect of NA inhibitors on liposome efficacy in this *in vivo* study was not significant. Additional studies are needed to better understand the degree by which viral neuraminidase affects glycan-labeled liposomes *in vivo*.

In addition to combining exogenous NA inhibitors with LSTc-labeled liposomes, we explored loading LSTc-labeled liposomes with the zanamivir in order to increase efficacy. Loading was accomplished by performing liposome extrusion in the presence of zanamivir solution. Both LSTc-labeled and unlabeled liposomes loaded with 200 µM zanamivir were generated and their ability to block PR/8 infection of MDCK cells was measured (**Figure 31**). Zanamivir encapsulated in the liposome greatly increased the efficacy of both unlabeled and LSTc-labeled liposomes in blocking influenza infection, and the zanamivir-loaded LSTc-labeled liposomes inhibited infection nearly completely. This again demonstrated the synergy of LSTc-labeled liposomes with current NA inhibitors. It also highlighted the potential of using the liposomal platform to specifically deliver small molecule therapeutics to virus.

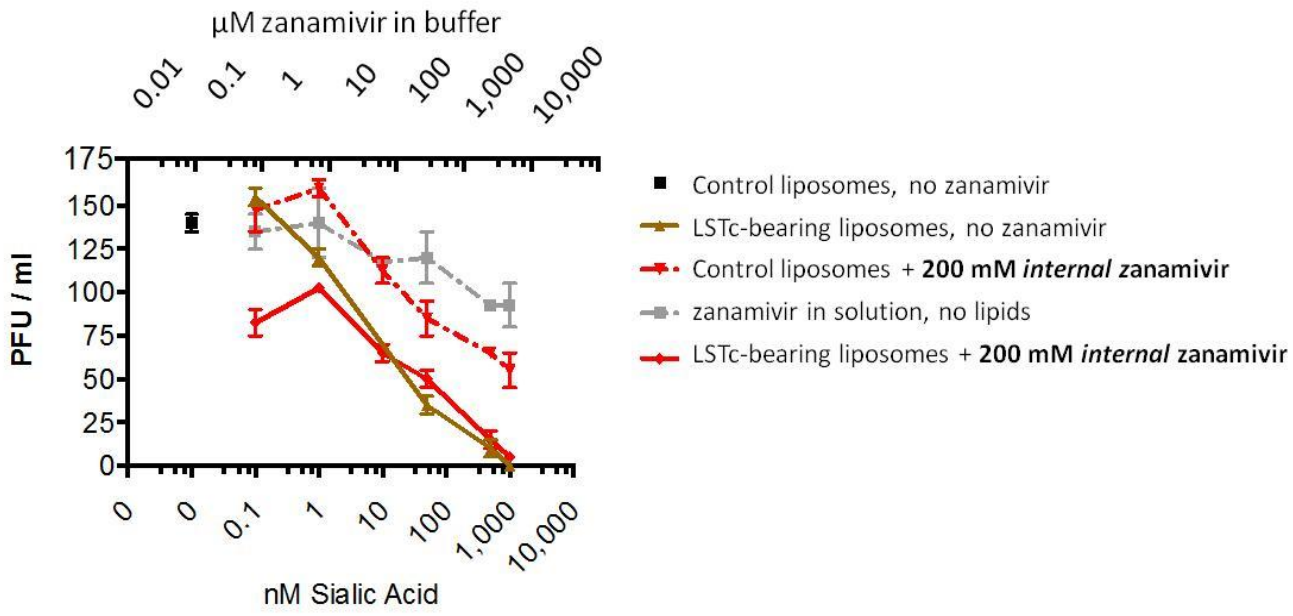

Figure 31. Efficacy of zanamivir-loaded liposomes. Liposomes with (green and purple bars) or without (orange and red bars) LSTc were untreated (orange/ green) or pre-loaded with 200 µM zanamivir (red/purple) then premixed with PR/8 for 30 minutes at 37C. The mixture was then added to MDCK cells for one hour and the PFU recovered after 48 hours was assessed.

If SA-glycan bearing liposomes are indeed adversely affected by influenza NA, it is possible to redesign the sialic acid linkage on LSTc (or LSTa, if needed) so that it is resistant to NA hydrolysis. This would entail use of a glycan with a different core that would be isolated then modified chemoenzymatically for NA-resistance. Purification of the glycan, modification, incorporation into glycolipid, extrusion into liposomes, and testing NA resistance and binding is a significant undertaking that will be reserved for later project stages if deemed necessary. A less attractive approach is to develop a dosing strategy where an NA inhibitor is co-administered with LSTc-labeled liposomes; this may be onerous if used in therapy.

HSocta-bearing liposomes

This HS-octasaccharide DOPE was the used in a pilot study to produce HS-octsaccharide bearing liposomes. Using the standard formulation used for LSTc-bearing liposomes (7.5 mol% glycolipid, 30% cholesterol, and 62.5% DOPC), extrusion of liposomes containing 7.5 mol% HS-octasaccharide DOPE through a 200 nm membrane produced 140 nm diameter liposomes that had the same general physical characteristics as similar batches of LSTc-bearing liposomes. These liposomes were found to be over 1000x more effective in inhibiting RSV infection of Vero cells than purified HS-octasaccharide in solution (unpublished). A 50% reduction in RSV infectivity was achieved with roughly 500 µM HS-octasaccharide in solution compared to 100 nM HS-octasaccharide on the surface of liposomes. This showed that display of the HS-octasaccharide on the surface of liposomes recreated the multivalent binding to the RSV F and G proteins and increased affinity to the RSV virion. We will next test different amounts of HS-octasaccharide on the liposome surface to see if we can improve *in vitro* activity versus RSV. We will then test efficacy in a mouse model of RSV infection, with HS-octasaccharide-bearing liposomes and RSV instilled via the intranasal route, and viral titers, cytokines, and

histopathology used as endpoints. Demonstration of the efficacy of anti-RSV liposomes is particularly promising since it is the HS-octasaccharide should be able to interact with and inhibit other virus, or it can be combined with LSTc or similar glycans on the liposome surface to increase the spectrum of activity. Another promising future direction is exploiting the immunomodulatory properties of heparin-derived glycans to combine their effect with anti-viral activity.

REFERENCES

Feldman SA, Audet S, Beeler JA. The fusion glycoprotein of human respiratory syncytial virus facilitates virus attachment and infectivity via an interaction with cellular heparan sulfate. J Virol. 2000 Jul; 74(14):6442-7.

Hendricks GL, Weirich KL, Viswanathan K, Li J, Shriver ZH, Ashour J, Ploegh HL, Kurt-Jones EA, Fygenson DK, Finberg RW, Comolli JC, Wang JP. Sialylneolacto-N-tetraose c (LSTc)-bearing liposomal decoys capture influenza A virus. J Biol Chem. 2013 Mar 22;288(12):8061-73.

Hope MJ, Bally MB, Webb G, Cullis PR. Production of large unilamellar vesicles by a rapid extrusion procedure: characterization of size distribution, trapped volume and ability to maintain a membrane potential. Biochim Biophys Acta. 1985 Jan 10; 812(1):55-65.

Krusat T, Streckert HJ. Heparin-dependent attachment of respiratory syncytial virus (RSV) to host cells. Arch Virol. 1997; 142(6):1247-54.